PURE ZINC AND ZINC/CERAMIC COMPOSITE COATINGS BY ELECTRODEPOSITION

PURE ZINC AND ZINC/CERAMIC COMPOSITE COATINGS BY ELECTRODEPOSITION

By

XULI XIA, B. E., M. Sc.

A Thesis

Submitted to the School of Graduate Studies

in Partial Fulfillment of the Requirements

For the Degree

Master of Applied Science

McMaster University

© Copyright by Xuli Xia, 2007

MASTER OF APPLIED SCIENCE (2007) McMaster University

(Materials Science & Engineering) Hamilton, Ontario

TITLE: Pure Zinc and Zinc/Ceramic Composite Coatings by Electrodeposition

AUTHOR: Xuli Xia, B. E., M. Sc. (University of Science and Technology Beijing, Beijing, China)

SUPERVISOR: Dr. Joseph R. McDermid

Dr. Igor Zhitomirsky

NUMBER OF PAGES: xii, 111

ABSTRACT

Pure zinc and zinc/yttria stabilized zirconia (YSZ) composite coatings for combined wear and corrosion protection of ferrous substrates were prepared by electrodeposition using acidic zinc sulphate solutions containing YSZ and gelatin. The morphology of the electrodeposit was studied by Field Emission Scanning Electron Microscopy (FESEM) with energy dispersive spectroscopy (EDS). X-ray diffraction was employed to determine the texture of the zinc deposits. In the electrodeposition of pure zinc coatings, the influence of electrodeposition parameters, including current density, deposition time and solution pH was studied. It was found that the deposition rate was controlled by the current density and that an increase in deposition time resulted in the formation of deposit microstructures with coarse, columnar grains. The deposits prepared from solutions with lower pH were composed of uniform, fine grains and exhibited a basal plane preferred orientation.

The effects of gelatin on zinc electrodeposition were investigated. It was found that the addition of gelatin profoundly modified the microstructure and crystallographic orientation of the zinc deposit. As the gelatin concentration increased, the mean grain size of zinc deposit was reduced and the basal plane preferred orientation was inhibited. The modification of the microstructure and orientation by gelatin increased microhardness of the zinc coating. However, the corrosion protection property which was assessed by potentiodynamic polarization test was not significantly changed.

In the study on composite coatings, the incorporation of ceramic particles in the zinc deposit was characterized as a function of the deposition solution composition. The effect of ceramic particles on the hardness of the composite coatings was assessed by microhardness. The corrosion potential of the composite coating was determined by potentiodynamic polarization tests. The results showed that decrease in solution pH and addition of gelatin promoted the co-deposition of ceramic particles with zinc. The mechanical and corrosion properties of conventional zinc coatings were improved by the incorporation of ceramic particles.

ACKNOWLEDGEMENTS

I would like to express my sincere appreciation to my supervisors, Dr. Joseph R. McDermid and Dr. Igor Zhitomirsky, for their valuable guidance and support throughout this research work. Their kind encouragement and patience are priceless to me during the course of my study in McMaster University.

My appreciation is also extended to Steve Koprich for his assistance in the FESEM operation and Chris Butcher for his advice on sample preparation in my experiments. I am very grateful to Florent Lefevre-Schlick for his friendly assistance in the work with EBSD.

Many thanks to all members of Dr. McDermid and Dr. Zhitomirsky's teams and to my friends in our department, Xin Pang, Lihua Chen, Erika Bellhouse, Jun Cao, Janice Wei, Marco Cheng and Tao Wu for their kind help and friendship.

At last but not the least, special gratitude goes to my parents. Their love and encouragement greatly support my life and study.

TABLE OF CONTENTS

LIST OF FIGURES

Chapter 2

Chapter 3

Chapter 4

Chapter 5

LIST OF TABLES

Chapter 2

Chapter 3

1 INTRODUCTION

Zinc based coatings have been widely used for the corrosion protection of ferrous materials. As a physical barrier, a layer of adherent zinc separates the substrate from the corrosive environment; the zinc layer also acts as an anode, offering self-sacrificial protection to the ferrous substrate. Electrodeposition has been utilized for zinc coating fabrication because of its uniformity and high purity of the product as well as the feasibility of depositing zinc layers on substrates with complex shapes. Being carried out under room temperature, electrodeposition effectively avoids the thermal attack characteristic of the hot-dipping[1] processes and retains the properties of the substrate steels obtained from previous process steps (typically cold rolling). Until 1970, zinc electrodeposition had been mostly performed in zinc cyanide electrolytes[2], but their toxicity limited further development of this technique and they were gradually replaced by acidic electrolytes.

Extensive research results have concluded that when working with acidic electrolytes, the morphology, crystal orientation and properties of the zinc coatings are very sensitive to electrodeposition process variables such as current density, electrolyte composition and solution pH. Thus, in a given electrodeposition system, it is important to determine the optimum working parameters. Among these variables, the addition of organic reagents has always been a concern. In the absence of organic additives, zinc deposits are normally coarsely crystalline and non-uniform. However, the addition of small amounts

of organic additives can considerably alter the morphology and properties of the deposit. Sitnikova and Sitnikov[3] studied the polarization effect of a group of organic dyes in a zinc chloride electrolyte. The addition of thiourea, dextrin, glycin and a mixture of them in a zinc sulphate electrolyte were investigated by Loto et al[4]. Franklin[5] and Oniciu et al[6] reviewed the mechanisms by which additives facilitate the deposition process. Generally, organic additives function through dirt blocking, ion bridging, ion pairing, interfacial tension modification, hydrogen evolution, hydrogen adsorption and electrode filming. Some additives may work via more than one mechanism. Many literature results show that in the presence of the organic additives, the quality of zinc coatings was improved. Bright and uniform zinc coatings with refined microstructures can be deposited from acidic electrolytes with the appropriate organic additives.

However, good quality or appropriate structures are not sufficient for zinc coatings in applications in aggressive environments. The service life of conventional zinc coatings are limited by corrosion attack and the relatively low wear resistance of the pure metal. Thus, composite coatings of zinc and ceramics with a combination of attractive properties of the various components have been developed to meet the requirements for protective coatings with long lifetimes and high corrosion resistance. Starting in the 1970's, various particles such as SiO_2[7], Al_2O_3[8] and TiO_2[9] have been included in the zinc matrix to increase the wear and corrosion resistance of the pure metal coating. Compared with other coating fabrication methods, co-deposition is considered to be a relatively simple and economic method to produce composite coatings of zinc and ceramic particles.

Through this approach, uniform composite coatings can be prepared directly from solutions with suspended particles on substrates with complex shape. However, successful deposition of composite coatings on the electrode depends on the preparation of stable suspensions of ceramic particles, which is difficult due to the high tendency of ceramic particles to agglomerate. On the other hand, theories of the co-deposition process have not been thoroughly investigated due to the complexity of the electrolyte systems and there are still many opportunities for the development of novel composite metal and ceramic coatings with unique properties.

Based on the above discussion, the present work undertakes to investigate the effects of operation parameters and gelatin on the microstructure and properties of zinc coatings in the electrodeposition process and to fabricate composite coatings of zinc and ceramic particles by co-deposition for the combined anti-wear and corrosion protection of ferrous materials.

The work presented in this thesis comprises five chapters:

1. Chapter 2 presents background information relevant to the work in this thesis, including basic definitions and factors in the metal electrodeposition process, the theory of electrophoretic deposition of ceramic particles and the co-deposition of metal and ceramic particles.
2. Chapter 3 describes the experimental materials, apparatus and procedure.
3. Chapter 4 presents the experimental results.

4. Chapter 5 includes analysis of the results and further discussion based on the mechanisms of electrodeposition.
5. Chapter 6 draws conclusions from the above and makes recommendations for further study.

2 LITERATURE REVIEW

2.1 Overview of Zinc Coatings

In recent decades the applications of steel products have ranged from large structures such as civil structures and power plants to automotive and appliance applications. The growth of the automotive industry has promoted a sharp rise in the consumption of steel all over the world. Since the utilization conditions for steel materials vary from mild environments to extremely aggressive ones, corrosion resistance has become an important requirement for steel products. Zinc coatings are commonly used in the corrosion protection of ferrous materials. It was reported[10] that the exterior body panels of vehicles made of zinc coated steels exhibited excellent anti-corrosion performance and significantly extended the service life of automobiles.

Zinc ranks fourth in tonnage of metal production and consumption in the world behind iron, aluminium and copper. Among its wide range applications, half of zinc products find application in protective coatings for ferrous materials. As a physical barrier, the zinc layer completely covers the substrate metal surface, separating them from the corrosive environment. In addition, located in less noble position than iron in the electromotive series of metals, zinc can also act as an anode and provide self-sacrificial protection to the underlying ferrous substrates if discontinuities such as voids, scratches, and cut edges take place in the coatings – this protection effect is also called galvanic protection. Furthermore, even after zinc coatings corrode and dissolve due to the galvanic

protection, the remaining zinc corrosion products can adsorb the oxygen[1], inhibiting the oxygen reduction reaction on the steel surface and reducing the corrosion rate.

Zinc based coatings are mainly fabricated by two technologies in industry: hot-dip galvanizing and electrodeposition. Hot-dip galvanizing is the oldest and most commonly used method. Zinc coatings produced from this technology are predominant in terms of production output and consumption in the world. In the galvanizing process, adherent coatings of pure zinc or zinc alloys are produced on iron or steel products by immersing the workpieces in a bath of molten zinc. The coatings formed by this method are chemically bonded to the ferrous substrates with a series of zinc-iron or iron-aluminium intermetallic layers and thus possess excellent adhesion.

Electrodeposition is another common method to produce zinc and zinc alloy coatings on steel products. The process of electrodeposition is also called electroplating or electrolytic deposition. To avoid confusion, we call this process electrodeposition in this project. It is defined as the deposition of metallic species onto a negatively charged electrode (cathode) by electrolysis[11]. The process can be considered an electrochemical reaction carried out by passing electric current through an electrolyte. In the electrodeposition process, positive ions migrate to the cathode under an applied voltage, becoming neutralized through charge transfer at the electrode and then these neutral metallic atoms are deposited on the cathode surface. Thus, in the process of zinc electrodeposition, zinc based coatings are formed on the steel cathode by reducing simple

zinc ions or zinc complexes from zinc salt electrolytes. Factors involved in the zinc electrodeposition process are discussed in the following sections.

2.2 Electrodeposition of Zinc

The zinc electrodeposition industry started in the early 20th century. Since the coating process is carried out at or close to room temperature, the abrupt heating and cooling attack induced by immersion in the molten zinc bath in the hot-dipping process can be effectively avoided. The properties of the steel substrate obtained from previous thermomechanical processing steps can also be retained. In the electrodeposition process, uniform coatings can be fabricated on one or both sides of the substrate with complex shape. The thickness of zinc deposit can be easily and rigidly controlled through varying the operating parameters. In addition, the high production rate and high purity of the deposit are also merits of the electrodeposition process over other coating production methods.

2.2.1 Electrolytes

In the industrial electrodeposition process, zinc coatings can be produced from different electrolytes. In term of composition, these electrolytes can be classified into two types: alkaline electrolytes and acid electrolytes. Alkaline electrolytes are largely cyanide solutions composed of zinc cyanide, sodium cyanide and sodium hydroxide, as shown in Table 2-1. The zinc cyanide provides zinc ions for deposition. The function of the sodium

hydroxide is to make zinc cyanide soluble by forming soluble complex hydroxyl salts[11]. In alkaline zinc electrolytes, zinc normally exists as complex ions. With superior throwing power, alkaline cyanide solutions can be used to produce uniform and bright zinc coatings on workpieces with irregular shape. It was also found that zinc cyanide electrolytes were the easiest to control among all of the zinc electrodeposition systems. Before the 1970's, zinc coatings deposited from cyanide zinc solutions were predominant in the market. However, the toxicity of cyanide solutions and their potential for impacting environment limited the utilization of this kind of electrolytes. The low production rate and high operating cost also generated more interest in acidic electrolytes.

In modern industry, acidic electrolytes are widely used in zinc electrodeposition for their advantages of low toxicity and capital investment. The most commonly used acid electrolytes are zinc sulphate solutions or zinc chloride solutions. The principal constituent of zinc sulphate electrolytes is zinc sulphate, which provides zinc ions for deposition. The higher solubility of the zinc sulphate in water allows for higher zinc ion concentrations in the electrolyte and thus increases the electrodeposition rate. The relatively low price of zinc sulphate is another reason to make this electrolyte widely used. A typical composition for zinc sulphate electrolytes is listed in Table 2-1.

Table 2-1: Composition of typical alkaline and acid zinc electrolytes[11]

Zinc Cyanide		Acid Zinc	
$Zn(CN)_2$	45-60 g/L	$ZnSO_4$	240-480 g/L
NaCN	90-150 g/L	NaCl	15-30 g/L
NaOH	90-140 g/L	H_3BO_3	20-100 g/L
Na_2CO_3	30-75 g/L	$Al_2(SO_4)_3.8H_2O$	25-35 g/L

The main component of zinc chloride-based electrolytes is zinc chloride which supplies both zinc ions for deposition and chloride ions to maintain the conductivity of the solution. Sodium chloride and aluminum chloride are included to increase electrolyte conductivity. The high conductivity of zinc chloride solutions allows them to be operated under high current density without agitation. Acetate electrolytes are also employed in zinc electrodeposition, although they are not used in large scale. Sekar and Jayakrishnan's reported that the acetate bath can be expected to be a minor ingredient in zinc electrodeposition baths for their non-polluting, non-toxic chemical properties[12]. The acetate-based bath also has advantages in obtaining bright deposits with higher cathode efficiency and low waste treatment cost.

The pH of the electrolytes is a very important factor that may affect the leveling, brightness and ductility of the deposit. In acidic electrolytes, the pH tends to increase due to the reduction of hydrogen ions at the cathode and this degrades the quality of the deposit. Thus, acid has to be periodically added to deposition electrolytes to keep the solution pH in the optimum range[13].

The reduction species in zinc deposition are different for acidic and alkaline solutions. In alkaline solutions, the deposition is accomplished via zinc complex ions. In most acidic electrolytes, zinc species exist in the form of simple ions and the deposition process is completed through two steps. The deposition rate is determined by the second reaction.

$$Zn \leftrightarrow Zn^{+} + e^{-}$$
$$Zn^{+} \leftrightarrow Zn^{2+} + e^{-} \quad (2\text{-}1)$$

2.2.2 Anodes

In zinc electrodeposition, two types of anodes are commonly used: soluble and insoluble anodes. It is obvious that the material of a soluble anode is pure zinc. Different grades of pure zinc are utilized as anodes for two purposes: maintaining the concentration of zinc ions in the electrolyte and supplying electrons for the reduction of metal on the cathode. During electrodeposition, zinc ions in the electrolyte are depleted due to continuous reduction and are replenished by dissolution of the anode. Thus, the deposition process is actually a transfer of zinc ions from the anode to the cathode through an aqueous media by the following two reactions:

$$\text{Anode: } Zn - 2e^{-} = Zn^{2+} \quad (2\text{-}2)$$

$$\text{Cathode: } Zn^{2+} + 2e^{-} = Zn \quad (2\text{-}3)$$

The drawbacks of the soluble anode in industry come from the dissolution of zinc anode by chemical corrosion when the electrolyte is not in operation[13]. The dissolved zinc can cause supersaturation of the electrolyte, adversely affecting the electrolysis operation. If operating with low purity zinc such as 98.5% or 99%, impurities in the zinc anode may result in degradation of the coating quality and prevent efficient operation of the deposition process. Therefore, the utilization of high purity zinc anodes is preferred in the zinc electrodeposition process.

The insoluble anode is adopted when there is special requirement for maintaining an even current distribution on cathodes with special shapes i.e. wire or workpieces with internal recesses[13]. However, insoluble anodes are not commonly used because additional zinc feeding is needed to keep deposition continuous.

2.2.3 Additives

In zinc electrodeposition, either in alkaline-based electrolytes or in acid-based electrolytes, one additive or the combination of several types of additives at small concentration is normally added. The addition of additives can inhibit the formation of coarse or dendritic crystalline structures, refine grain size, modify the texture of the deposit, control gas evolution, reduce gas pits and internal stress of the coating, enhance the brightness and improve levelling[6]. The microstructure may be dramatically changed by the addition of such additives, usually organic compounds. Many research works have concentrated on the effects of additives and their operating mechanism. Franklin reviewed the operation mechanisms by which additives affect the electrodeposition process[5]. These additive agents work by blocking the surface, changing the overpotential, ion pairing, forming complexes, modifying interfacial tension and affecting hydrogen evolution behaviour. Some additives act by more than one mechanism.

As grain refiners, additives act as dirt and attach themselves to the surface of the electrode or growing crystals, forming an insulating layer on these surfaces and slowing down the deposition process[14]. On the atomic scale, additives inhibit crystallographic

growth by either preferentially adsorbing at the growing edges or covering the whole surface. The adsorption of the foreign molecules can induce disorder in the incorporation of zinc atoms into the lattice, or block the diffusion of the atoms towards the growing centre of the deposit, resulting in the decrease of growth rate.

The formation of small grains depends on a lower rate of individual crystal growth and a higher nucleation rate which is exponentially related to the cathode overpotential based on Boltzman's equation[15]. The presence of additives in the electrolyte may cause variation in the potential of the electrodes. Thus, the refinement effect of some additives can contribute to the variation of cathode overpotential. Coverage of the electrode by additive molecules can increase the effective current density, and consequently increase the overpotential of the electrode. For cathodic deposition, the specific cationic adsorption moves the potential negatively, and the overpotential is increased. On the other hand, anionic adsorption will decrease the overpotential and possibly retard surface diffusion and inhibit deposition on the cathode[16]. Ohgai et al. [17] concluded that the addition of polyethylene glycol (PEG) shifted the zinc deposition potential in the less noble direction.

Additives can also decrease the roughness of the deposit forming smoother and brighter surface[18]. The adsorption of the surfactant takes place preferentially on the protrusions of the growing surface, converting the deposition of metal to the recessed areas. Fine grains and high overpotential are necessary for the leveling of the deposit. The presence

of additives in electrolytes usually enhances the growth rate of different crystal planes and results in the formation of deposits with preferred orientation[19]. The enhancement effect is attributed to that additives preferentially increasing the overpotential of certain crystal planes and then consequently increase their nucleation rate, which results in the growth of these crystal planes significantly faster than others. The crystal texture will be discussed in section 2.2.4.

It is well known that in acidic electrolytes the primary secondary reaction is the reduction of hydrogen ions at the cathode surface. If hydrogen is adsorbed on concave areas or in crevices, it would increase the coating roughness or result in hydrogen embrittlement of the substrate. The reduction of hydrogen ions or the adsorption of gas bubbles on the electrode surface occupies the activated sites on the cathode surface, resulting in a decrease in current efficiency. With the presence of additives, the hydrogen reduction rate is altered[5]. The adsorption of additives on the cathode surface can also change the surface activity and the mobility for removing hydrogen[5].

Commonly used additives in zinc electrodeposition include dextrin, thiourea, glycerol, gelatin and so on. Loto and Olefjord[20] investigated the effects of dextrin, thiourea, glycin and combinations of these additives on zinc crystallization from acid chloride solutions, and they found that the morphology of zinc deposit was profoundly modified and a non-porous coating was promoted by the addition of these organic agents. Song and Kim's investigation showed that polyethylene glycol (PEG), gelatin and thiourea

inhibited hydrogen evolution and adsorption during zinc electrodeposition from zinc sulphate solutions[21]. In alkaline zinc solutions, it was reported that the addition of glycerol can increase the free zinc ion concentration and catalyze zinc deposition[22]. Significant refinement of the grain size of zinc crystals was obtained by Youssef et al.[14] in the preparation of zinc coatings by pulse electrodepositition in the presence of polyacrylamide (PAA). With an increase in PAA concentration, the grain size of zinc deposit decreased to the nano-scale.

Gelatin, an organic polymer, is a widely used additive in zinc electrodeposition for leveling and brightening. Commercially available gelatin is prepared by the thermal denaturation of collagen, isolated from animal skin and bones, with very dilute acid. It can also be extracted from fish skins. In terms of structure, gelatin contains a large number of glycine (almost 1 in 3 residues, arranged every third residue), praline and 4-hydroxyproline residues[23]. In acidic solutions, it is hydrolyzed to form amino terminal groups with positive charge[24,25]. Used in cathodic metal electrodeposition, gelatin normally serves as a grain refiner[24, 25].

2.2.4 Crystalline Orientation of Zinc Deposits

The crystalline structure and preferred orientation of zinc deposits are critical to coating properties. When produced by electrodeposition, the structure and orientation of the deposit will vary in different electrolysis systems. The principle orientation planes for

zinc hexagonal crystal structures include the basal plane (0001), prism plane $(10\bar{1}0)$ and pyramid planes $(10\bar{1}1)$ and $(10\bar{1}2)$. In general, the basal plane is preferred for higher corrosion resistance and the prism and pyramid planes show better mechanical properties[28]. The development of microstructure and orientation can be controlled by changing the composition of the electrolyte, the operating conditions and crystal structure of the substrate. Alfantazi and Dreisinger's research[26] on the orientation of zinc deposits from industrial sulphate-based electrolytes indicated that with an increase of zinc concentration in the electrolyte, the deposit texture changed from a (0002) basal plane preferred orientation to a random orientation. Yim and Hwang[27] reported that higher current density promoted the development of non-basal planes and changed the orientation of basal planes non parallel to the substrate surface. Lindsay[28] found that the basal plane orientation changed from parallel to perpendicular to the substrate surface with variations in the solution pH. Substrate texture has a profound influence in the orientation of the deposited crystals. In thick coatings, deposits with preferred orientation are normally formed on randomly oriented polycrystalline substrates and amorphous substrates due to the competitive growth mode. While on the single-crystal substrates, the epitaxial growth mode is strongly enhanced[19].

The effect of additives on preferred orientation is complicated with considerable work having been devoted to it. Kondo et al. reported that (0002) hexagonal platelets were parallel to the substrate surface in the presence of Sn additive, while without additives,

the $(10\bar{1}0)$ planes became parallel to the substrate surface[29]. The development of deposit crystalline texture can be explained by the preferred nucleation and growth of certain crystalline faces. If the energy for the nucleation of a particular plane is smaller than for others, preferred orientation of this plane develops[15]. The adsorption of foreign atoms or molecules on the activated sites of the cathode surface can alter the cathode overpotential, redistribute the ion concentration in the area close to the cathode, and then affect the nucleation and growth mode.

Preferred orientation greatly changes the quality and properties of the coatings. For zinc protective coatings the corrosion resistance is the focus of concern. Many results show that the (0002) basal plane exhibited better corrosion resistance and lower corrosion current than others[28, 30]. Park and Szpunar[30] found that the corrosion current decreased with an increase in the basal texture intensity because having a higher binding energy of surface atoms, the close packed planes exhibited the highest dissolution resistance.

2.3 Electrophoretic Deposition (EPD) of Ceramic Particles

2.3.1 Introduction

As discussed above, zinc coatings offer excellent protection for ferrous materials against corrosion. However, the service life of conventional zinc coatings is limited by the aggressive environments and low mechanical properties of conventional zinc coatings. Particularly in recent years, the need for properties such as long durability and low

environmental pollutant level has promoted the rapid growth of materials with low cost and environment friendly natures. Advanced coatings such as ceramic or organic films with high anti-corrosion properties and high wear resistance are under development. So far, a wide variety of techniques have been employed in the production of novel coatings, including the sol-gel method[31], plasma spraying, electrodeposition, physical, chemical and electrochemical vapour deposition. Among these techniques, the electrophoretic deposition process (EPD) is considered to be a relatively simple technique for the fabrication of ceramic and organic coatings directly from particle suspensions. Compared with other methods, this method is a versatile one and can be modified easily for specific applications. The process of electrophoretic deposition of ceramic particles and the important factors influencing the process are discussed in the following sections.

2.3.2 Electrophoretic Deposition of Ceramic Particles

Electrophoretic deposition is a colloidal process, by which charged ceramic particles are dispersed in a liquid medium, migrate and deposit onto an oppositely charged substrate under the force of a DC electric field[32]. Two types of EPD process are employed in the preparation of ceramic films based on which electrode deposition occurs: (i) cathodic electrophoretic deposition where the particles are positively charged and deposited on the cathode and (ii) anodic electrophoretic deposition, in which the particles are negatively charged and the deposition occurs on the anode. These two types of electrophoretic deposition process are schematically illustrated in Figure 2-1.

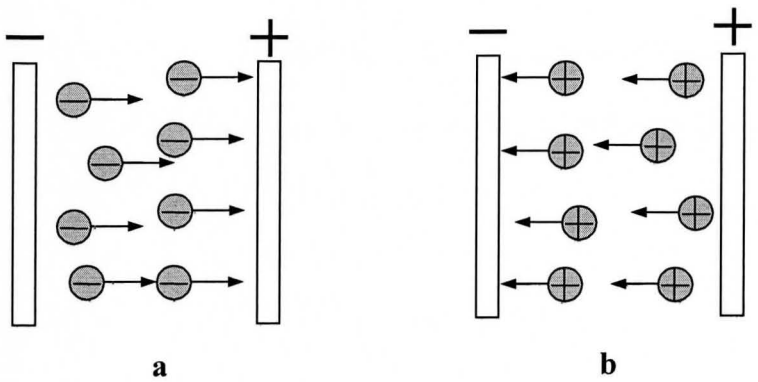

Figure 2-1: Schematic illustration of electrophoretic deposition process: (a) anodic EPD and (b) cathodic EPD

2.3.3 Particle Charging and the Mobility of Particles

In the EPD process, successful accumulation of ceramic particles on the electrode is achieved via the electrophoretic motion of the charged particles in the liquid medium. The prerequisites to form a homogeneous ceramic layer are the preparation of a stable and well dispersed suspension of charged ceramic particles and the development of sufficient surface charge on the ceramic particles[33]. These two factors are also crucial to the thorough understanding of the EPD mechanism.

As solid ceramic particles are added to a liquid medium, they can acquire surface charge and the redistribute ions in the vicinity, i.e. attracting ions with opposite charges (counter ions) towards the solid surface and repelling ions with the same charge (co ions) away from the particle surface leading to the formation of the so-called electric double-layer.

Many investigations[34, 35] have been focused on the determination of the exact distribution of electrical charge near particle surface. According to the Stern model[19], the double-layer consist of a compact Stern layer and a diffusion layer. The Stern layer was composed of counter ions and was located in the plane of the centers of fixed hydrated ions. It represented the closest distance that a hydrated counter ion can approach the solid particle. The outer diffusion layer was defined from the Stern layer to the bulk of the solution. The structure of the double layer and its potential is schematically shown in Figure 2-2.

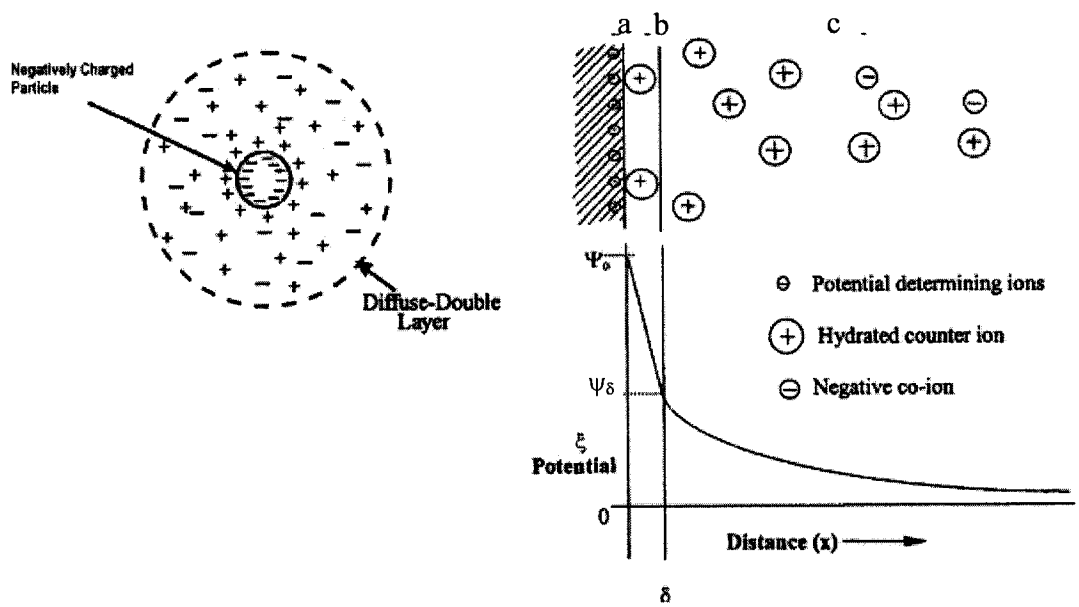

Figure 2-2: Schematic representation of the double layer and potential drop across the double layer: a-surface charge, b-Stern layer, c-diffuse layers of counter-ions[36]

Derived from the one-dimension Poisson equation, the potential decayes exponentially across the double layer as expressed in the equation:

$$\psi(x) = \psi_\delta \exp(-\kappa x) \tag{2-4}$$

The thickness of the double layer is designated as the distance where the potential drop to 1/e of the potential at the Stern plane (ψ_δ), thus the thickness of double-layer is equal to 1/κ, also called the Debye length. At room temperature, the double layer thickness in aqueous solutions can be expressed as:

$$\frac{1}{\kappa} = \left(\frac{\varepsilon \varepsilon_0 kT}{e^2 \sum n_i z_i^2} \right)^{1/2} \tag{2-5}$$

Here, e is the electronic charge, n_i is the concentration of ions with charge z_i, ε is the dielectric constant of the liquid, ε_0 is the permittivity of a vacuum and T is temperature. The double layer thickness is very important to the stability of suspensions since it determines the range of double layer repulsive force and thus affects the total potential energy of particles.

The development of surface charge on particles is normally represented by the zeta potential (ζ) which is designated as the potential difference between the Stern layer and the diffuse layer in Figure 2-2. The definition of zeta potential is based on the migration of a charged particle in an electrolyte under the effect of an applied voltage. As seen from Figure 2-2, a charged particle in the suspension is surrounded by counter ions with higher concentration than that in the bulk solution. Under an applied voltage, rather than move to the opposite direction, a fraction of these counter ions move together with the particle due to the attraction force of the particle. The speed of a moving particle is determined by

the net charge of the whole liquid sphere that moves along with the particle. The potential at the sphere surface or the Stern surface is the so-called zeta potential. Therefore the zeta potential plays a very important role in determining the direction and speed of the suspended particles. According to electrophoretic theory[37], the velocity of a solid particle in suspension is related to the zeta potential via the following equation:

$$v = \mu E \tag{2-6}$$

$$\mu = \frac{2\varepsilon\varepsilon_0\zeta}{3\eta} f(\kappa a) \tag{2-7}$$

Where, v is velocity of a particle in suspension, μ is the electrophoretic mobility of the particle, ζ is the zeta potential, ε is the dielectric constant of the solvent, ε_0 is the vacuum dielectric permittivity, and η is the viscosity of the liquid. The $f(\kappa a)$ function is related to the double layer thickness and the particle dimensions.

The mechanism of charge development on the particle surface varies in different kinds of solvents. In aqueous suspensions, particle surface charge can develop through four mechanisms as follows[35]: (a) selective adsorption of ions onto the solid particle from the liquid, (b) dissociation of ions from the solid phase into the liquid, (c) adsorption or orientation of dipolar molecules at the particle surface and (c) electron transfer between the solid and liquid phases due to differences in work function. Particles in the polar liquid, such as water, tend to coordinate water molecules to form hydroxylated surfaces, and obtain positive or negative charge. The net charge formed by the following reactions is controlled by the pH of the liquid[32]:

$$M-OH+H^{+} \Leftrightarrow M-OH_2^{+} \quad (2\text{-}8)$$

$$M-OH+OH^{-} \Leftrightarrow M-O^{-}+H_2O \quad (2\text{-}9)$$

The point of zero charge (pzc) is the pH value at where the surface concentrations of M-OH^{+}_2 and M-O^{-} are equal. Particles are negatively charged at pH>pH_{pzc} and positively charged at pH<pH_{pzc}.

In non-aqueous solvents, where there is no water and the hydration effect is scarce, surface charge on ceramic particles is achieved via various mechanisms. One possibility is electron transfer between the particles and the solvent[34]. Similar to the pH scale in aqueous solutions, the tendency of a non-aqueous solvent to donate electrons or to accept electrons is represented by the donor and acceptor numbers- i.e. the donicity of the solvent[34] The donicity of a solvent is given by the enthalpy of reaction with an arbitrarily chosen reference acid[38]. It was found that the particle surface charge changed sign at a particular value D_{NO}. If a solvent had donicity D_N>D_{NO}, it contributed electrons to the solid particles, result in the formation of a negative charge on the particles. Conversely, in a solvent having donicity D_N<D_{NO}, solid particles tended to loose electrons and become positively charged[38]. Another possible way for particles to obtain surface charge is through the adsorption or desorption of ions. Investigation of Wang et al.[39] showed that alumina particles obtained surface charge by adsorption of protons or hydroxyls in ethyl alcohol.

2.3.4 Stability of Suspensions

The successful production of a homogeneous ceramic film in the electrophoretic deposition process depends on the achievement of a well stabilized, unagglomerated, and homogeneous suspension. The suspension behaviour is strongly influenced by interparticle/surface forces. Interparticle forces in suspensions include (a) coulombic double-layer repulsion, (b) van der Waal's attraction[40,41], (c) volume exclusion effects in suspension with higher particle concentration[42] and (d) steric (polymeric) forces[43]. The suspension stability depends on the total interparticle potential energy determined by all of these forces.

2.3.4.1 DVLO Theory

One widely accepted theory for the stability of suspensions is the classical DLVO theory. Established by Derjaguin and Landau[40] and Verwey and Overbeek[41] this theory quantitatively relates the stability of suspensions with particle interaction energies. In the DLVO theory, the liquid is assumed to be stationary and the collision of particles results from Brownian motion. The stability of the suspension is determined by the total interaction energy between particles where the interaction between particles consists of electrostatic repulsion (V_R) and van der Waals attraction (V_A).

The attraction energy can be expressed as:

$$V_A = -\frac{A}{6}\left(\frac{2}{s^2-4}+\frac{2}{s^2}+\ln\frac{s^2-4}{s^2}\right) \qquad (2\text{-}10)$$

Here, A is Hamaker constant which is related to the ionic strength, s=2+D/a, D is the shortest distance between two particles and a is the particle radius.

The electrostatic repulsion energy is:

$$V_R = 2\pi\varepsilon\varepsilon_0 a\psi^2 \ln\left(1+e^{-\kappa D}\right) \tag{2-11}$$

where, ψ is the surface potential, $1/\kappa$ is the double-layer thickness, D is the distance between two interacting particles, ε is the dielectric constant of the solvent, ε_0 is the vacuum dielectric permittivity and a is the particle radius.

The total energy of interaction (V_{total}) is the combination of these two effects and can be expressed as:

$$V_{total} = V_R + V_A \tag{2-12}$$

Thus, the total interaction potential energy can be expressed as a function of the distance between particles as depicted in Figure 2-3.

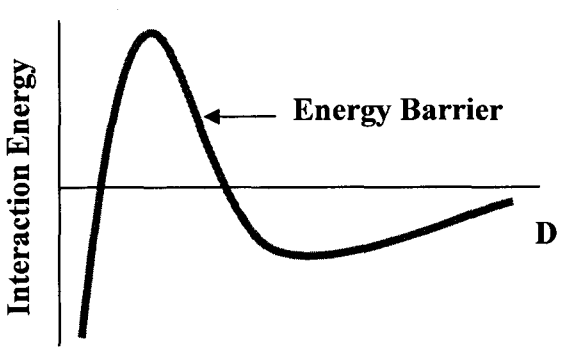

Figure 2-3: Total potential energy versus interparticle distance[32]

When the diffusion layer repulsion is comparable to the van der Waal's attraction, the total energy curve exhibits a maximum value. This peak represents a potential energy barrier against the contact of the two particles, and it has critical role in coagulation. It is clear that if particles tend to come into close contact, they have to possess sufficient energy to overcome the energy barrier for coagulation. The height of the potential energy peak depends on the magnitude of the surface charge and the range of repulsive forces i.e. the thickness of the double layer. The ψ item in the equation 2-13 indicates that higher surface charge is a necessary to form a higher repulsion force between particles. Since in suspensions of solid particles, the surface charge is normally represented as the zeta potential (ζ), developing high zeta potential on particles in suspension is a prerequisite for keeping the suspension stable.

Another factor determining the energy barrier is the range of repulsive force, which is strongly influenced by the double layer thickness. It is demonstrated and shown in Figure 2-4 that as the electrolyte concentration increases, the double layer becomes thinner, and the height of energy barrier decreases due to the double layer overlap. In electrolytes with very high ion concentration, the repulsion effect vanishes completely.

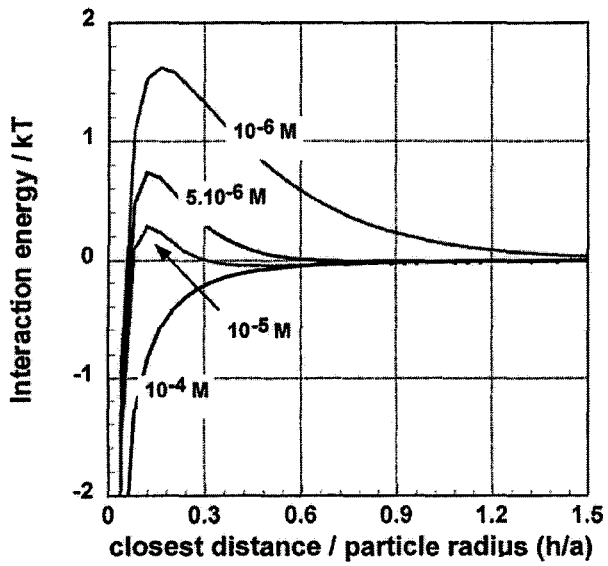

Figure 2-4: Interaction energy between two particles surrounded by a double layer for a surface potential of 25 mV, a particle radius of 0.35 μm, a Hamaker constant of 10^{-20} J, and a relative dielectric constant of 20 for various concentrations of a background electrolyte[33].

2.3.4.2 Other Effects on Suspension Stability

The DLVO theory can only deal with a dilute suspension. Only two interactions were considered to influence the coagulation of particles. In fact, however, many other types of interparticle forces in a colloidal system have to be considered. As particle concentration increases, the volume exclusion effect will result in a higher tendency for particle coagulation[42]. In some cases, steric stabilization induced by the addition of additives in the suspensions may vary the magnitude of surface charge and significantly influence the dispersion behaviour of colloidal particles. It was found that acids may act as dispersants and promote the development of surface charge[44]. Many reports[44, 45] indicate that the zeta potential of ceramic particles can be controlled by the variation in the pH of suspensions. A schematic relation between zeta potential and suspension pH is shown in

Figure 2-5. Therefore, to achieve sufficient surface charge more consideration need to be taken on the operation pH range in the EPD processes of ceramic particles.

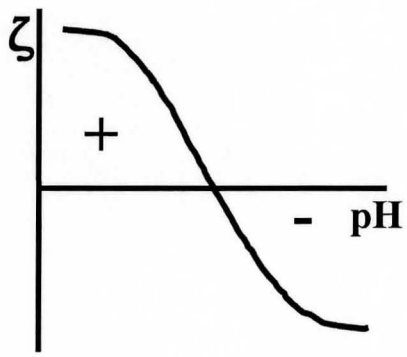

Figure 2-5: Zeta potential of ceramic particles versus pH of suspension[32]

Many inorganic ions and organic polyeletrolytes have been utilized to induce steric stabilization via adsorption to the particle surface and have resulted in repulsion between these macromolecules. The particle stabilization is schematically illustrated in Figure 2-6.

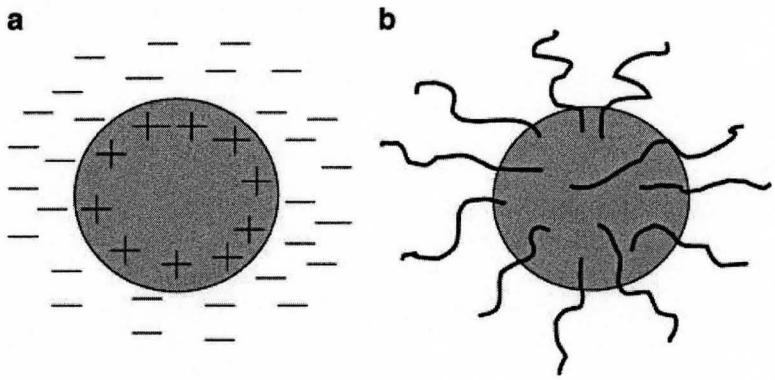

Figure 2-6: Schematic illustration of (a) electrostatic stabilization (b) steric stabilization of suspensions[46]

In the EPD process, particle size is also an important factor closely related to the stabilization of suspensions. If the particles for deposition are too large, it will be difficult to obtain sufficient surface charge to overcome the effect of gravity. Particles will precipitate on the bottom of the suspension. Small particles, however, easily agglomerate due to strong interparticle interactions. From the above discussion on the interaction between particles, it is known that repulsion forces decrease with particle dimensions. Moreover, particles with small diameter exhibit high surface energy and tend to contact to reduce the total surface area. Nanoparticles, due to Brownian motion, can not settle down at the electrode under lower electric field. Therefore, difficulties are related to the formation of nano-structured deposits [47]. But it does not mean the electrophoretic deposition of nanoparticles is unfeasible. In fact, EPD has already been employed for preparation of nano-structured films[48]. Giersig[49] is the first to use EPD to prepare ordered monolayers of gold nanoparticles.

2.4 Co-deposition of Composite Coatings

The above discussion reviewed the electrodeposition process for pure metals and ceramic particles respectively. In some practical applications, superior ductility and easy accessibility make metallic coatings predominant in the market for protective coatings. Furthermore, metal-based coatings are preferred for the relatively small difference in thermal expansion coefficients of metal coatings and steel substrates. Many investigations have been undertaken on the development of composite coatings of metal

and incorporated second phases with unique electrochemical and mechanical properties[50,53,54].

Composite coatings are often fabricated by the co-deposition of metal and ceramic particles. It is a process by which small ceramic particles with micro or nano dimensions are suspended in a metal salt solution and co-deposited with the metal atoms. The co-deposition process is actually a combination of the electrolytic deposition of metal ions and the electrophoretic deposition (EPD) of ceramic particles. Therefore, the advantages and problems in these two processes are imparted to the co-deposition technique as well. Since key factors these processes have been discussed, the following paragraphs are focused on the electrodeposition characteristics of composite coatings and the mechanism of the co-deposition.

2.4.1 Advanced Composite Coatings

The research in composite coatings of metal and ceramic or organic polymer particles began in the 1960's and has increased substantially during the last decade. The properties of composite coatings depend on the species of incorporated particles and the proper combination of ceramic and metal phases. The unique properties of composite coatings come from the properties of particles dispersed in the bulk metal matrix or from the particles partially embedded in the coating surface. Metal-based composite coatings were developed originally to improve corrosion resistance, mechanical properties and wear resistance. Hard particles such as oxides[50], carbides[51] and diamond[52] were

incorporated into metallic films for dispersion strengthening and higher abrasion resistance. For example, the addition of Al_2O_3 particles significantly improved the wear characteristics of nickel films[53]. Incorporation of ZrO_2 nanoparticles was also reported to greatly increase the hardness of nickel coatings[54]. In composite coatings, the metal matrix acts as a ductile binder to hold the hard second phase, while the hard phase carries higher mechanical loads and imparts resistance to abrasion[55].

In the development of coatings for corrosion protection, various particles such as SiO_2[56], Al_2O_3[8] and TiO_2[57] have been included in the zinc matrix to increase the wear and corrosion resistances of the pure metal coating. It was shown by Aslanidis et al. that the improved corrosion property of zinc and SiO_2 composite coatings came from not only the dispersion effect of particles in the bulk of the metal coatings but also the interlocking effect of particles on the coating surface with the top paint layer[58]. Good paint adhesion was promoted by the association of silane compounds of the silica particles with terminal groups in the polymeric paint layer. SiO_2 particles were also reported to improve the corrosion resistance of zinc coatings by supporting the corrosion productions [59]. With progress in the field of advanced ceramic materials, CeO_2, Y_2O_3, and ZrO_2 particles have been utilized in the preparation of multi-functional composite coatings[60] such as thermal barrier coatings, electrochemical and optical films. These materials exhibit excellent structure and chemical stability at high temperature as well as higher thermal shock resistance and higher toughness and hardness[61]. Particularly the superior anti-oxidation nature of these ceramic particles makes them widely used as protective coatings in

corrosive or elevated temperature environments. It was reported that the incorporation of zirconia particles significantly decreased the corrosion rate of nickel coatings at 1073 K and 1173K[62].

2.4.2 Co-deposition Mechanism of Metals and Solid Particles

Although the co-deposition process has obtained a wide range of practical applications, investigations on the theory or mechanism of this technique progress at a slow rate. Based on the current understanding of the process variables, two models, namely the Guglielmi model[63] and MTM model[64], show better agreement with experimental results and have been widely accepted.

2.4.2.1 Guglielmi Model

The Guglielmi model is an important step in the theoretical investigation of the mechanism of co-deposition. In this model the co-deposition process was completed via the two steps of adsorption and the capture of ceramic particles in the growing metal deposit was due to electrophoretic attraction. In the first step, a particle is surrounded by a layer of ions and solvent molecules physically adsorbed on the electrode surface. The adsorption is very loose and there is no real contact between the electrode and particle. In the second step, under the influence of electric field, the particle is strongly adsorbed to the electrode, the double layer outside it uncovered and the particle irreversibly captured by the cathode. This model was consistent with results in the co-deposition of various

systems: alumina with nickel, TiO_2 with copper from copper sulphate solution and so on. However, since only two parameters, current density and particle concentration in the electrolyte, were incorporated, this model showed considerable deviation from many experimental results and failed to predict the effects of operation variables on the deposition process.

2.4.2.2 MTM Model

The MTM model proposed in 1987 was aimed at predicting the amount of incorporated particles. This model was based on two fundamental postulates[64]:

1. An adsorbed layer of ionic species is created around ceramic particles once they are added to the solution.
2. The reduction of some of these adsorbed ionic species is necessary for the incorporation of particles into the metal matrix.

In the MTM model, the composite coating was collected through the five steps illustrated in Figure 2-7:

i. Adsorption of ionic species on the particle surface
ii. Migration of particles towards the electrode under the influence of the electric force
iii. Diffusion of particles across the diffusion double layer
iv. Adsorption of particles with the surrounding ionic cloud on the electrode surface
v. Reduction of some adsorbed ions by which particles were irreversibly entrapped by the metal matrix.

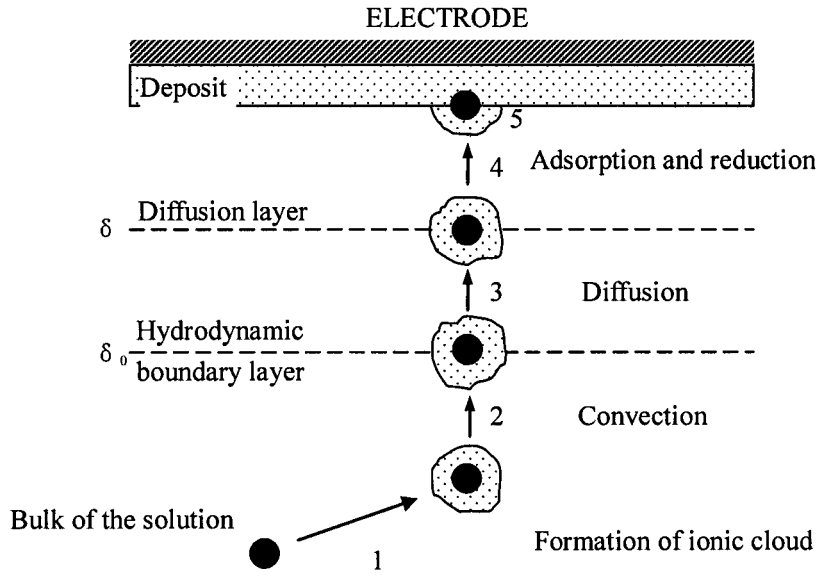

Figure 2-7: Five steps in the co-deposition of particles[64]

Since many interactions between particles and ionic species in the electrolyte and variables in the process are not incorporated in the present model, more general mathematical models that can better predict the deposition behaviour are still under development.

2.5 Objectives of the Present Study

Based on the above discussion concerning the electrodeposition of zinc-based coatings, the quality, electrochemical and mechanical properties of conventional zinc coatings can be significantly improved by additives and dispersed second phases. Advanced protective

coatings are required for long service life and application in aggressive environments. The objectives of the work in this thesis are to address the following points:

1 Study the effects of the variables on the quality of deposit fabricated via zinc sulphate electrolytic deposition.

2 Investigate the effects of an organic additive, gelatin, on the characteristics and properties of electrodeposited zinc coatings.

3 Develop novel zinc and ceramic coatings with advanced electrochemical and mechanical properties using the co-deposition technique.

4 To characterize the composite coatings and assess the coating's electrochemical and mechanical properties.

3 EXPERIMENTAL METHODS

3.1 Experimental Materials

AISI 301 stainless steel foils (Shim In a Can) with dimensions of 50×50×0.1 mm were used in the electrodeposition experiments as the cathode substrates to support the zinc deposit. The stainless steel foil used in this study had a polycrystalline microstructure with preferred orientations of (001), (002) and (211) for ferrite and (002) and (022) for austenite, as shown in Figure 3-1.

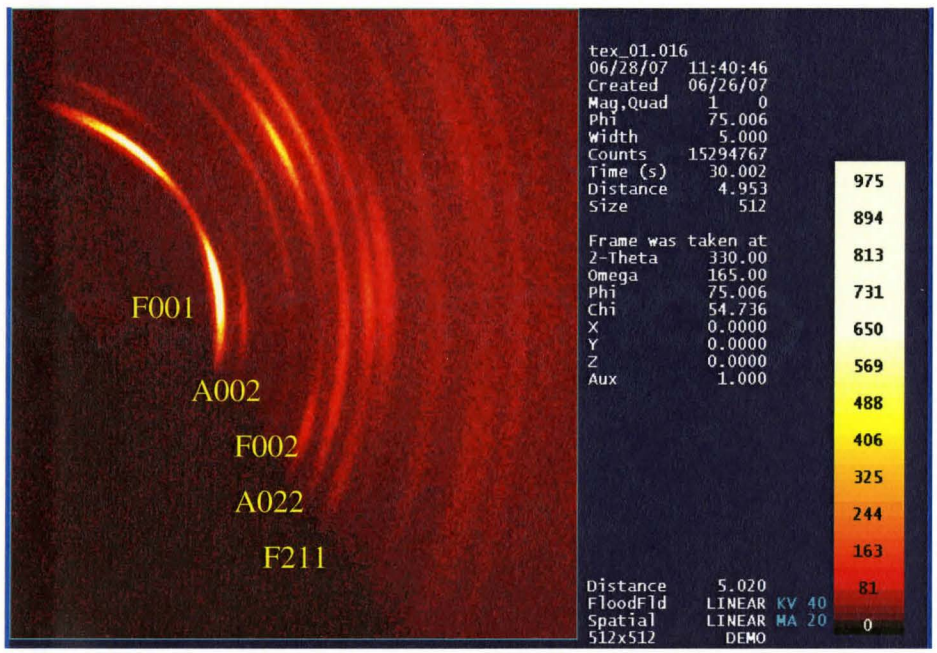

Figure 3-1: X-ray diffraction pattern of the stainless steel substrate

High purity (99.99%) zinc sheets with a dimension of 60×50×1 mm from Alfa Aesar were used as soluble anodes to supply zinc ions for deposition and maintain a constant zinc ion concentration in the electrolyte.

Table 3-1: Electrolyte compositions used in experiments

Electrolytes	Composition	
A	$ZnSO_4.7H_2O$	201.3 g/L
	Na_2SO_4	35.2 g/L
	NaCl	15.7 g/L
	pH	5 and 3
B	$ZnSO_4.7H_2O$	201.3 g/L
	Na_2SO_4	35.2 g/L
	NaCl	15.7 g/L
	Gelatin	0.5-6mg/L
	pH	5 and 3
C	$ZnSO_4.7H_2O$	201.3 g/L
	Na_2SO_4	35.2 g/L
	NaCl	15.7 g/L
	YSZ	2g/L-15g/L
	pH	5 and 3
D	$ZnSO_4.7H_2O$	201.3 g/L
	Na_2SO_4	35.2 g/L
	NaCl	15.7 g/L
	Gelatin	2 mg/L
	YSZ	2-15 g/L
	pH	3

Four electrolytes (A, B, C, D) were used for the electrodeposition of pure zinc and composite zinc/ceramic coatings. The electrolyte compositions are listed in Table 3-1. Aqueous solutions of zinc sulphate, sodium sulphate and sodium chloride were used to prepare electrolyte A, which was used as a base electrolyte throughout this work. The

chemical agents purchased from Caledon Company were of analytical grade (>99%). 10 vol% sulphuric acid (Caledon) was used to adjust the pH of the electrolytes.

Electrolytes C and D were utilized to produce composite coatings of zinc and ceramic particles. An aqueous solution of gelatin (45 wt%) from Norland was used as the additive. 8 mol% yttria stabilized zirconia particles from TOSOH with a specific surface area of 7 ± 2 m^2/g were added to the zinc sulphate electrolytes at concentrations from 2 g/L to 15 g/L. The morphology of an YSZ particle before electrodeposition is shown in Figure 3-2.

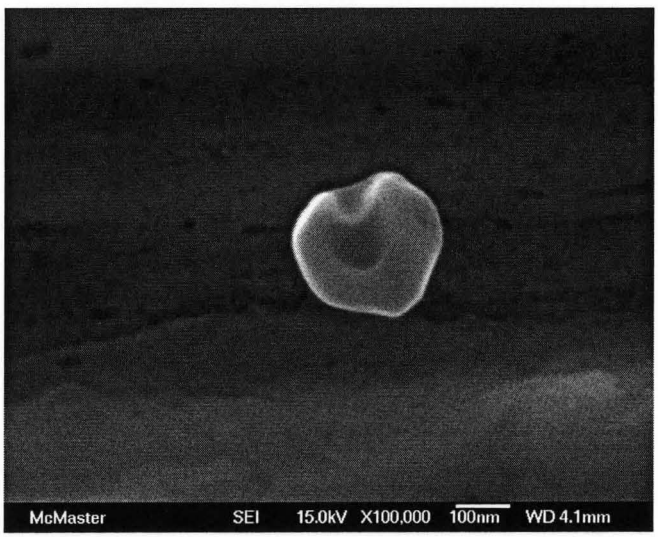

Figure 3-2: SEM image of YSZ particle before electrodeposition

3.2 Electrodeposition Apparatus

The apparatus for electrodeposition experiments is schematically shown in Figure 3-3 and consisted of one stainless steel cathode and two pure zinc anodes parallel to each

other. The deposition current and voltage were supplied via a power supply, electrophoresis EPS 601 (Amersham Biosciences), as shown in Figure 3-4. Within the operating range of 600 V, 400 mA, 100 W, the power supply can work under constant voltage, constant current or constant power modes. The process parameters including deposition time, current density and applied voltage were input from the control panel. The power supply can stop automatically and alarm at the end of a run, realizing precise control of the experiment. In this project, the constant current mode was used to maintain a constant deposition rate through out the deposition process.

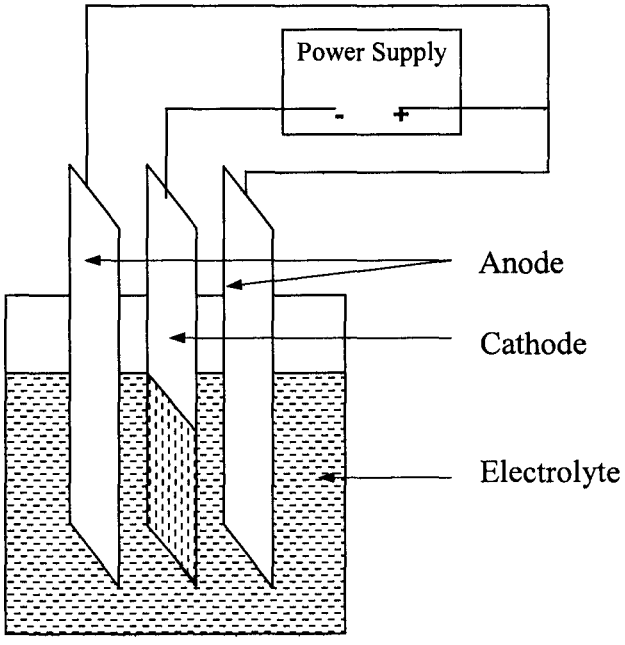

Figure 3-3: Schematic of electrodeposition apparatus

Figure 3-4: Electrophoresis power supply – EPS 601

3.3 Experimental Procedure

Pure zinc coatings and composite coatings of zinc and yttria stabilized zirconia (YSZ) ceramic particles were prepared by cathodic electrodeposition from zinc sulphate-based electrolytes. All deposition experiments were carried out at room temperature $(25 \pm 2°C)$ in the parallel electrode cell, as shown in Figure 3-3. Two zinc anodes and one steel cathode were fixed to a sample holder made of teflon, dipped into the electrolyte and connected to the electrophoresis power supply. The substrate area in contact with the electrolytes was 40×50 mm and was 50×50 mm for the zinc anode.

Throughout the electrodeposition processes, the electrolytes were stirred at a speed of 300 rpm to maintain a constant zinc ion concentration in the vicinity of the cathode and remove gas bubbles formed by the reduction of hydrogen ions at the cathode. For co-

deposition experiments, the magnetic stirring also had an agitation function to prevent ceramic particles from precipitating from the suspension. After electrodeposition, the deposit was rinsed with deionized water, cleaned with acetone and dried with a warm air stream.

3.3.1 Substrate Preparation

In order to remove grease and dirt from the substrate, a surface treatment was carried out prior to each deposition. Stainless steel foils were degreased with a 2 vol% sodium hydroxide solution at room temperature and were then polished with emery paper from 200 to 1200 grit. Between each polishing step the stainless steel foils were rinsed with deionized water. After polishing, the foils were cleaned with isoproponal in an ultrasonic cleaner for 20 mins, rinsed with acetone, and dried in a warm air stream.

3.3.2 Electrolyte Preparation

Electrolytes for electrodeposition were prepared by dissolving zinc sulphate, sodium sulphate and sodium chloride in deionized water under magnetic stirring. The pH value of the deposition electrolytes was adjusted with 10 vol% sulphuric acid, after the chemicals were completely dissolved. The solution pH was varied from 5 to 3.

The liquid gelatin solution was diluted to a 0.45 wt% aqueous solution with deionized water and was stabilized at pH 2 with 10 vol% sulphuric acid to prevent regelling.

Different volumes of this solution were added to the electrolytes to determine the effect of this additive.

In the deposition of composite coatings, 8 mol% yttria stabilized zirconia particles were added to the electrolyte, stirred for 30 mins and dispersed with ultrasonic oscillation for 1 hour.

3.3.3 Deposition Parameters

The electrodeposition of the zinc and zinc-ceramic composite coatings was carried out under various conditions. Some important process parameters for electrodeposition: deposition time, current density and electrolyte pH were varied as listed in Table 3-2. The concentration variations for the additives and the YSZ ceramic particles in the electrolytes are also shown in Table 3-2.

Table 3-2: Process parameters for the electrodeposition

Deposition Time (min)	Current Density (mA/cm^2)	pH	Concentration of gelatin (mg/L)	Concentration of YSZ (g/L)
5-60	10, 20, 30	5, 3	0, 0.5, 1, 2, 3, 4, 5, 6	2, 5, 10, 15

3.4 Characterization Methods

3.4.1 FESEM with EDS

A JSM-7000F Field Emission Scanning Electron Microscope (FESEM) equipped with Energy Dispersive Spectroscopy (EDS) was used to observe the surface and cross-sectional morphology of the deposits. FESEM was also used to investigate the distribution of ceramic particles in the directions parallel and perpendicular to the substrate surface. EDS point and elemental mapping analysis were employed to identify the ceramic (YSZ) phase. The distribution of YSZ ceramic particles normal to the substrate surface was studied by EDS elemental line scans.

3.4.2 X-ray Diffraction

A Bruker D8 powder X-ray diffractometer was used to analyze the crystallographic preferred orientation of deposits under different experimental conditions. Monochromatic Cu-K_α radiation was used at a scanning rate of 1 degree per minute through the range of 2θ from 20 to 75 degrees. Peaks in the X-ray diffraction pattern were identified according to the JCPDS files (Joint Committee on Powder Diffraction Standard) database of standard zinc powder sample. The preferred orientation of the deposits was calculated from the X-ray diffraction pattern by comparing the ratio of the relative intensity of basal (0002) to pyramid face $(10\bar{1}1)$ with the value calculated according to the standard powder sample database. The basal preferred orientation in our case was represented with an index, R, which was calculated from the equation:

$$R = \frac{\dfrac{I^{D}_{(0002)}}{I^{D}_{(10\bar{1}1)}}}{\dfrac{I^{S}_{(0002)}}{I^{S}_{(10\bar{1}1)}}} \tag{3-1}$$

Here, I^D is the relative diffraction intensity of the electrodeposited sample and I^S is the relative diffraction intensity of the standard zinc powder sample. Thus, a randomly oriented sample would have an R value equal to 1 and a sample with a basal plane preferred orientation would exhibit R>1.

3.4.3 Electron Backscattered Diffraction (EBSD)

The Electron Backscatter Diffraction detector on the JSM-7000F Field Emission Scanning Electron Microscope was used to study the effects of processing parameters on the morphology and preferred orientation of crystallites in the deposit. The HKL Channel 5 Flamenco data processing software was used to analyze the data and calculate the pole figures.

EBSD is a surface technique, with the diffraction signal coming from the top few nanometers of the material. Thus, the samples have to be polished to obtain a flat surface. As the thickness of the zinc coatings was typically 10 μm, the sample polishing process could not follow the conventional sample preparation steps for EBSD and moreover, to avoid corrosion, zinc coatings have to be polished in a non-aqueous environment. Thus, samples for EBSD analysis were only lightly polished using a suspension of 50 nm

alumina powders in 80 vol% ethanol and 20 vol% glycerol followed by cleaning with acetone.

The mean grain size of the zinc deposit was determined by the Mean Linear Intercept method according to the ASTM standard[65]. In this technique, the mean grain size is determined by laying a series of uniformly distributed test lines on a planar section and counting the number of grains that are intercepted.

$$L_M = \frac{L_T}{N_T \cdot M} \tag{3-2}$$

Where L_M is the mean diameter of grains, L_T is the total length of the test lines, N_T is the total number of the grains intercepted by the test lines and M is the magnification.

3.4.4 Microhardness

Vickers microhardness of the pure zinc and zinc/ceramic composite deposits was measured using a LECO M-400-H2 hardness testing machine with a square diamond indentor. A load of 10 g was used. Twenty measurements with a separation of 1 mm between indentations were carried out on each sample. The quoted microhardness of the sample was the average of 20 measurements.

The Vickers microhardness of coatings was calculated as follows[66]:

The shape of the indenter shown Figure 3-5 is a square-based pyramid with an angle of 136° between opposite faces (22° between the indenter face and surface). The Vickers Pyramid Number (H_V) is determined by the equation:

$$H_V = \frac{F}{A} \approx \frac{1.854F}{d^2} \tag{3-3}$$

Where, the F is the applied force and A is the surface area of the resulting indentation, determined by:

$$A = \frac{d^2}{2\sin\left(136°/2\right)} \approx \frac{d^2}{1.854} \tag{3-4}$$

Here, d is the average length of the diagonal and can be calculated as $d = (d_1 + d_2)/2$, d_1 and d_2 is the measured length of the indentation diagonals.

The maximum indentation depth was calculated using the geometrical relationship:

$$Depth_{max} = \frac{d_{max}}{2\tan 22°} \tag{3-5}$$

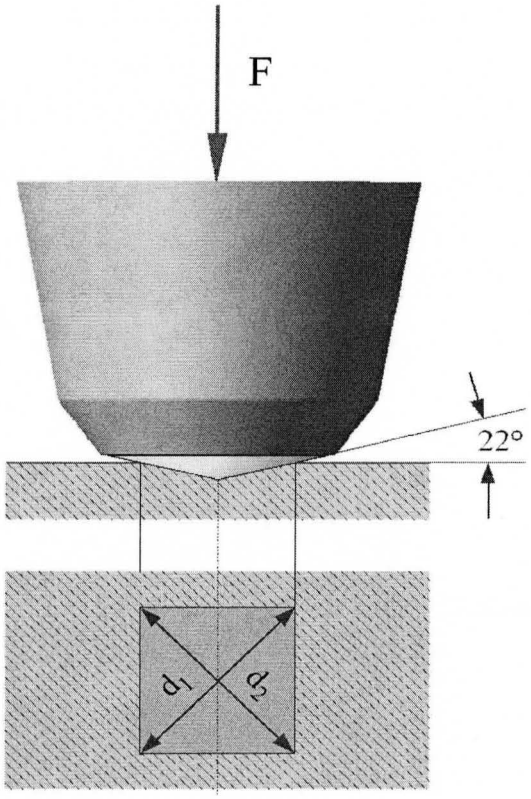

Figure 3-5: Vickers hardness test scheme

3.4.5 Potentiodynamic Polarization Test

The corrosion potential of the pure zinc and composite coatings was determined by potentiodynamic polarization testing at room temperature. The tests were performed using a Princeton PARSTAT 2273 advanced potentiostat system with a three-electrode cell. Fresh and clean deposits were cut into 16 mm diameter discs and set as the working electrode with a test area of 100 mm^2. The reference electrode, which was a Saturated Calomel Electrode, was connected to a salt bridge with the tip of a capillary tube. The reference electrode was set very close to the testing area of the sample with a separation

of less than 2 mm. Platinum mesh was used as the counter electrode. Potentiodynamic polarization tests were carried out in the range of ±250 mV from the open circuit potential vs. SCE at a scan rate of 1 mV/s and the response current recorded.

The electrolyte for the potentiodynamic polarization testing was a solution of 5 wt% sodium chloride in deionized water. Prior to testing, the electrolyte was de-aerated with high purity nitrogen gas for 1 hour and the atmosphere of nitrogen gas maintained throughout the test to minimize the effect of oxygen on the polarization behaviour of the coatings. Three measurements were performed on samples prepared under the same electrodeposition conditions.

3.4.6 Cathode Overpotential

Galvanostatic polarization of stainless steel substrates in electrolytes containing different concentrations of gelatin was undertaken to study the effect of gelatin on the cathode polarization behaviour. The cathode potential was measured as a function of gelatin concentrations in the pH 3 zinc sulphate electrolyte under a constant current density of 20 mA/cm^2. The working electrode for this test was freshly polished stainless steel foil. The apparatus was the same three-electrode cell used in section 3.4.5.

3.4.7 Cathode Polarization Test

Cathode polarization tests of the stainless steel substrate were performed in the same apparatus as that used in section 3.4.5. Freshly polished stainless steel foils were

polarized from their open circuit potential to -2.0 V versus SCE at a scanning rate of 2 mV/s and the response current recorded.

Six solutions used for the cathode polarization tests were classified into two groups whose compositions are listed in Table 3-3.

Table 3-3: Solutions for the cathode polarization tests

Group 1	$ZnSO_4.7H_2O$ 201.3 g/L Na_2SO_4 35.2 g/L NaCl 15.7 g/L	pH=5
		pH=3
		pH=3 with 2 mg/L gelatin
Group 2	$ZnSO_4.7H_2O$ 201.3 g/L Na_2SO_4 35.2 g/L NaCl 15.7 g/L YSZ 5 g/L	pH=5
		pH=3
		pH=3 with 2 mg/L gelatin

4 RESULTS

4.1 Characterization of Pure Zinc Coatings

In the process of electrodeposition, operating parameters normally have significant influence on the quality of the deposit. To investigate the effects of process variables on zinc electrodeposition, the current density, deposition time and pH value of the electrolyte were varied. The morphology and crystallographic orientation of the resultant zinc coatings were characterized by SEM and X-ray diffraction.

4.1.1 Effects of Current Density and Deposition Time

In studying the effects of current density and deposition time, the deposition experiments were performed in the pH 5 electrolyte. The current density and deposition time were varied per Table 3-2. Figure 4-1 shows the specific deposit mass versus deposition time under different current densities. It is seen that under a given current density, deposition proceeded at a constant rate and the deposit weight increased linearly with deposition time. The deposition rate increased with current density.

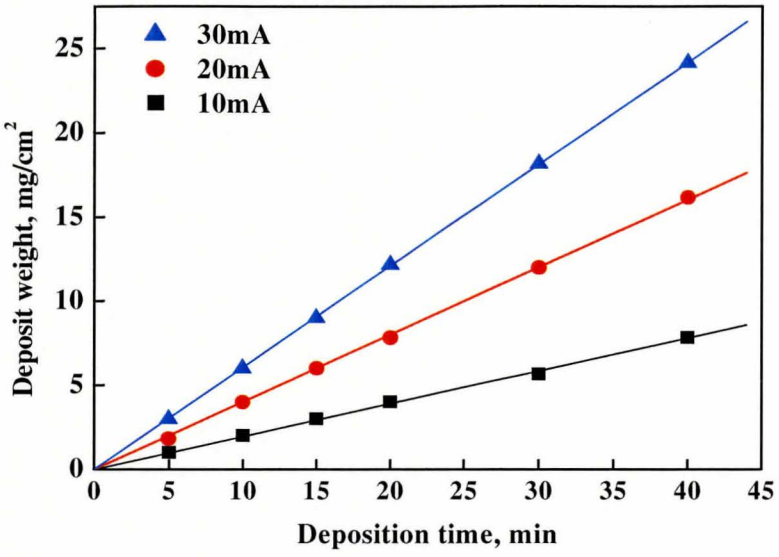

Figure 4-1: Deposit weight versus time in pH 5 electrolyte under various current densities

The morphology of the deposit prepared at each experimental current density was observed via FESEM and the mean grain size of the deposit measured and the results shown in Figure 4-2. The results show that the grains size of the zinc deposit increased with current density and deposition time. Figure 4-3 shows examples of zinc deposit morphology. The samples were prepared at current density of 20 mA/cm^2. It can be seen from the cross-sectional image, Figure 4-3 (d), that the zinc deposit evolved from a uniform fine grained morphology to a coarser columnar microstructure.

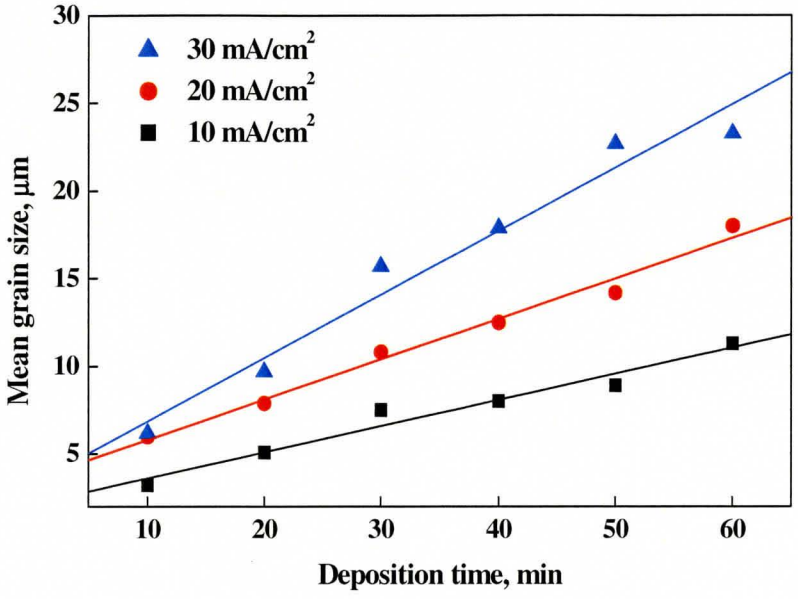

Figure 4-2: Mean grain size of zinc deposits versus deposition time in pH 5 electrolyte under various current densities

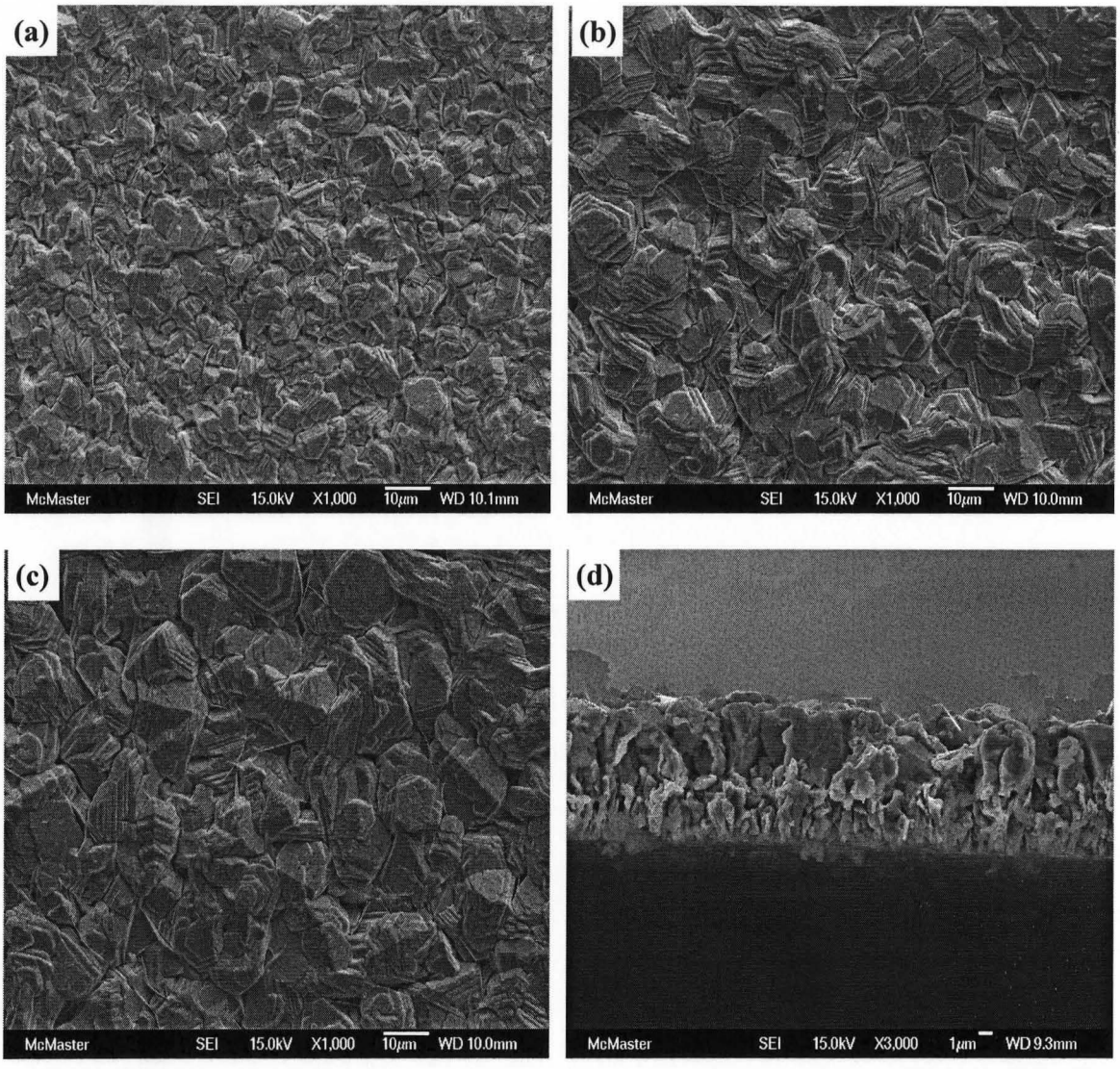

Figure 4-3: Surface morphology of pure zinc coatings electrodeposited using pH 5 electrolyte at 20 mA/cm^2 for (a) 20 mins, (b) 40 mins, (c) 60 mins and (d) cross section of the sample in (a)

Current density and deposition time also had an effect on the preferred orientation of the zinc deposit. The orientation of the zinc deposit was assessed by the ratio of basal plane (0002) to pyramid plane $(10\bar{1}1)$ X-ray peaks, which was defined via equation 3-1 in

Chapter 3. The results are shown in Figure 4-4. It can be seen that as the current density and deposition time increased, the basal plane (0002) became more predominant and the growth of prism plane $(10\bar{1}1)$ was constrained i.e. the crystalline structure tended to exhibit a strong basal plane preferred orientation nearly parallel to the substrate surface.

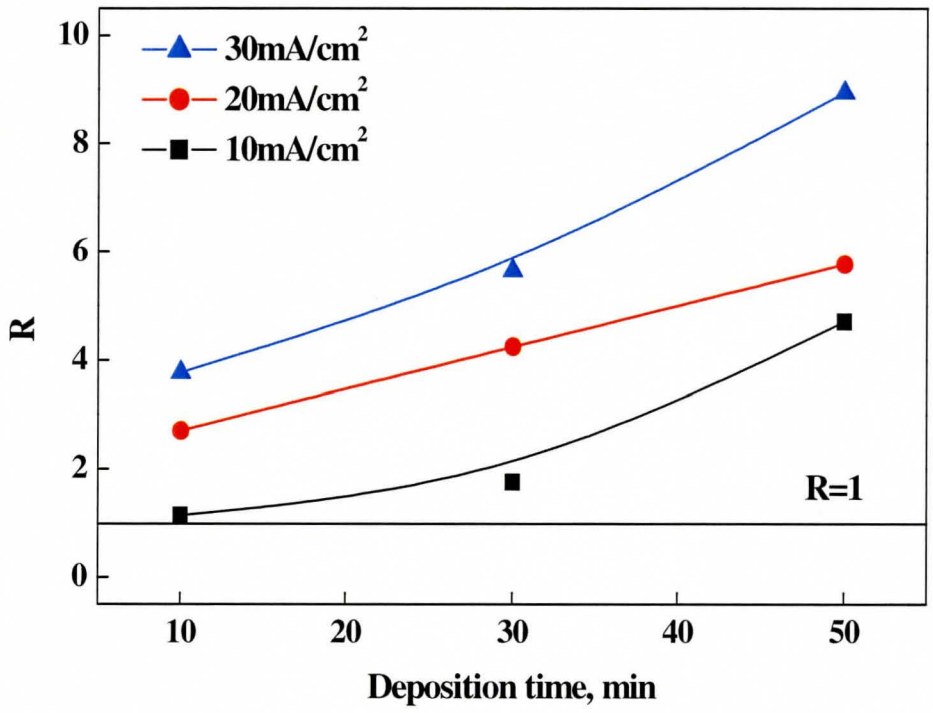

Figure 4-4: X-ray intensity ratio of (0002) to $(10\bar{1}1)$ versus deposition time under various current densities

4.1.2 Effects of Electrolyte pH

The pH value of the electrodeposition electrolyte is very important in determining the quality and properties of the coating. In the present study, the pH values were varied from 5 to 3 and current density and deposition time were fixed at 20 mA/cm^2 and 20 mins, respectively.

The morphology of the zinc deposit produced from electrolyte A with different pH values was observed with the SEM, as shown in Figure 4-5. The coating prepared from the solution with pH 3 was composed of finer and more densely packed grains. However, strong hydrogen evolution in the acidic solution resulted in the formation of gas pits in the zinc deposit.

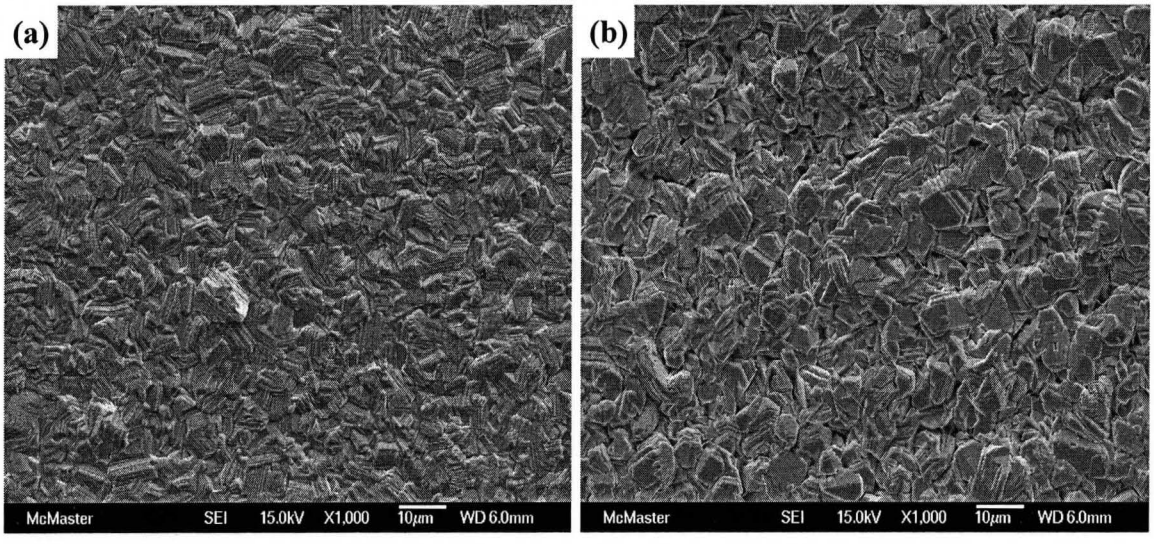

Figure 4-5: Effect of electrolyte pH on deposit morphology (a) pH=3, (b) pH=5 at 20 mA/cm^2 for 20 mins

The preferred orientation of the deposits changed significantly with electrolyte pH. As shown in Figure 4-6, growth of the basal plane (0002) was strongly enhanced by the addition of acid, and the growth of pyramid faces $(10\bar{1}0)$, $(10\bar{1}1)$ and $(10\bar{1}2)$ was inhibited. In the zinc deposit prepared using electrolyte with pH 3, the microstructure was composed of the basal plane which was preferentially oriented nearly parallel to the substrate surface.

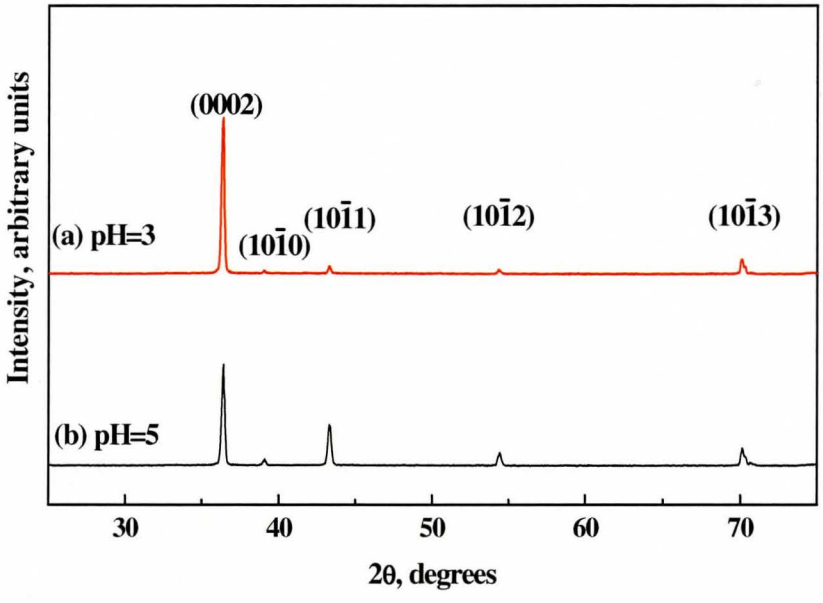

Figure 4-6: X-ray diffraction patterns of zinc deposits at pH=3 and pH=5, deposition time 20 mins and current density 20 mA/cm^2

The corrosion potential of coated and uncoated samples was assessed by potentiodynamic polarization in a 5 wt% sodium chloride solution. Figure 4-7 illustrates that the zinc

coatings had a more negative corrosion potential than the ferrous substrate. Thus, when corrosion occurred, zinc worked as an anode to prevent dissolution of the substrate. Figure 4-7 also indicates that zinc coatings prepared from the pH 3 electrolyte exhibited a more positive corrosion potential than those prepared using the pH 5 electrolyte.

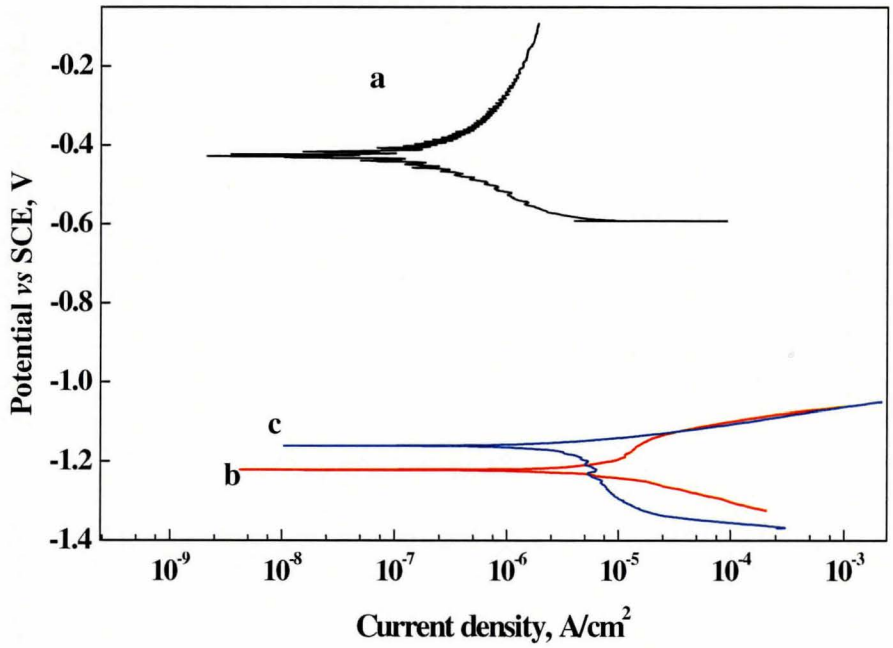

Figure 4-7: Potentiodynamic polarization curves (a) uncoated stainless steel and zinc coatings prepared from electrolytes with (b) pH 5 and (c) pH 3

4.2 Characterization of Zinc Coatings Prepared from Electrolytes Containing Gelatin

Small amounts of organic additives are normally used for the purpose of improving the morphology of the deposit. In this study, the effects of gelatin on the zinc electrodeposition process were investigated. The deposition experiments were performed in the pH 5 and pH 3 electrolytes, under current density of 20 mA/cm^2 for 20 mins. The morphology of the deposit and preferred orientation of the zinc coatings with addition of gelatin were characterized by FESEM, X-ray diffraction and EBSD.

4.2.1 Morphology of Zinc Coatings

The effect of gelatin on the coating morphology was investigated using SEM and EBSD. Coatings were prepared from electrolyte B with a deposition time of 20 mins. In the electrolyte with pH 5, the zinc deposition process, as shown in Figure 4-8, was retarded by the addition of gelatin. The coating exhibited an inferior morphology and did not cover the substrate uniformly. Thus, the addition of gelatin in pH 5 electrolytes showed no positive effect.

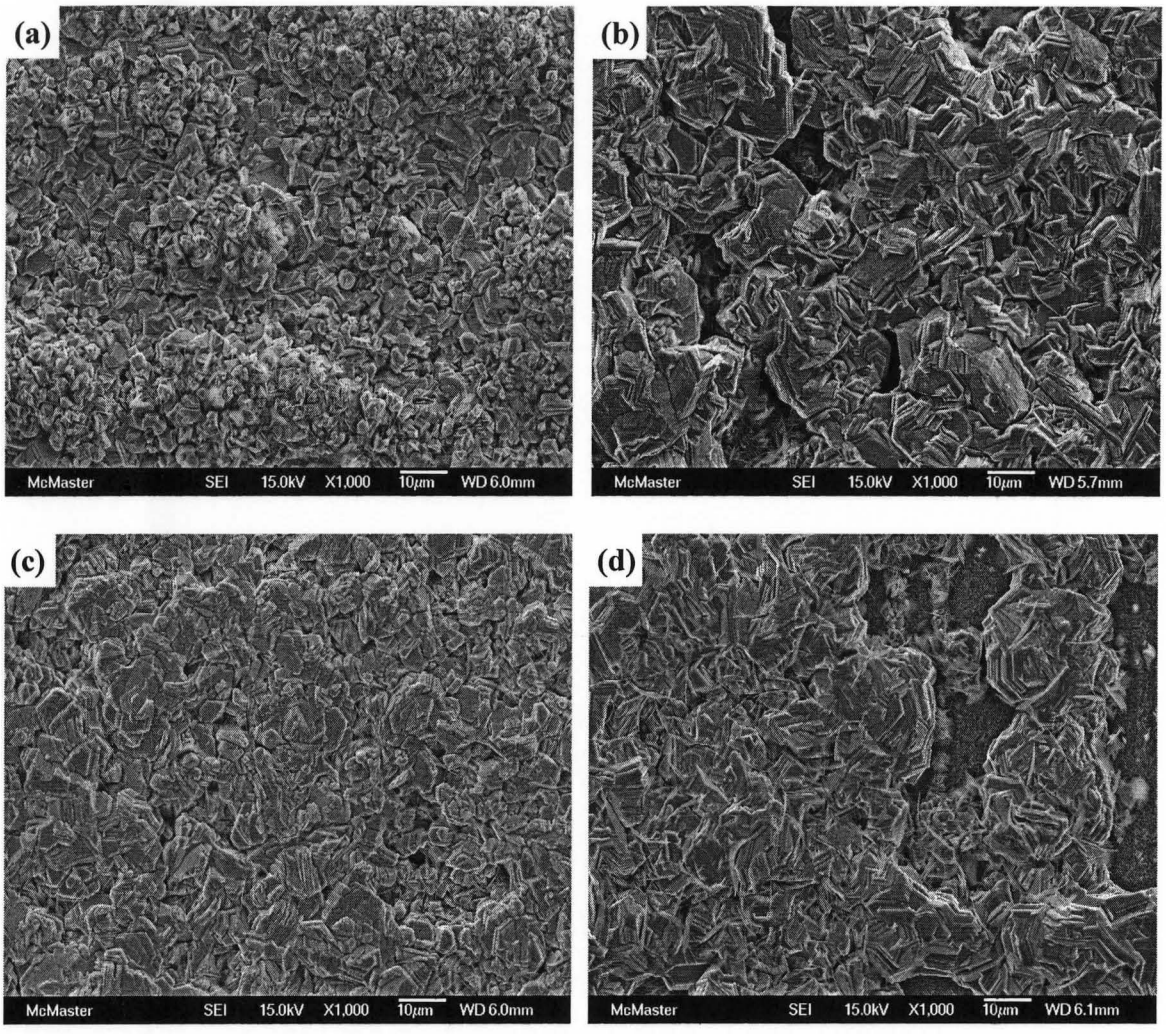

Figure 4-8: Zinc coatings from pH 5 electrolytes containing various amounts of gelatin: (a) 0.5 mg/L, (b) 1 mg/L, (c) 3 mg/L and (d) 5 mg/L

For the coatings prepared using pH 3 electrolytes, as the gelatin concentration increased two features with bimodally distributed grain sizes appeared in the deposit, as shown in Figure 4-9: (i) densely packed small zinc grains which covered the substrate uniformly and (ii) large-sized ridge-like grains which grew out from the normal fine grains.

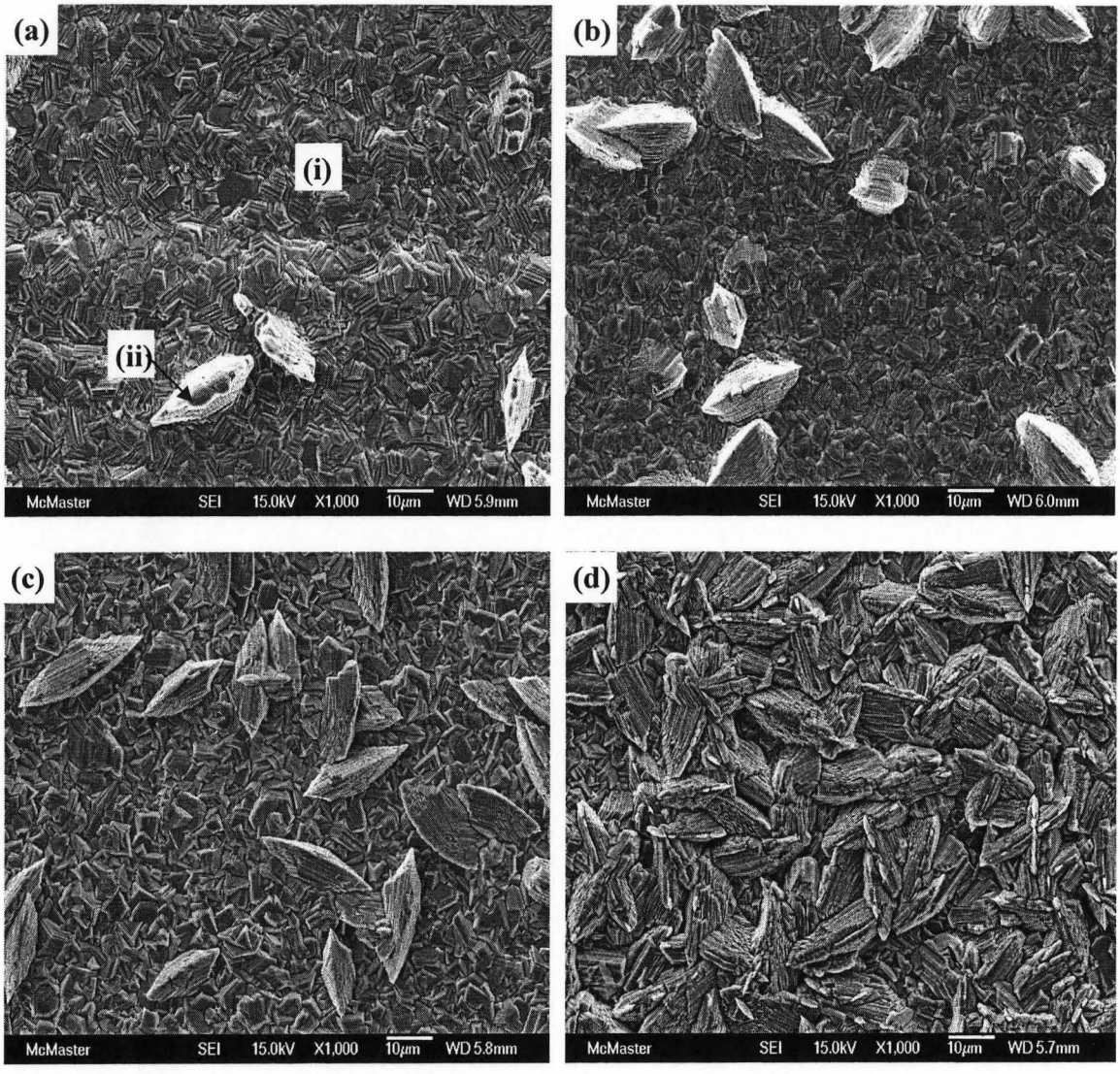

Figure 4-9: Zinc coatings from pH 3 electrolytes containing various amounts of gelatin: (a) 0.5 mg/L, (b) 2 mg/L, (c) 5 mg/L and (d) 6 mg/L

For the densely packed features, each grain was composed of many zinc layers with common orientation which were nearly parallel to the substrate surface. The zinc grain size decreased with increasing gelatin concentration. On the other hand, as the concentration of gelatin increased, some regions of the deposit developed abnormally as

ridge-like features growing out from the deposit surface as shown in Figure 4-9. The number of these ridge-like features increased with the concentration of gelatin, as can be seen by comparing Figure 4-9 (a) and Figure 4-9 (d). As the concentration of gelatin increased, the ridge –like features grew larger and extended to cover the entire surface of the deposit. The zinc layers consisting of the ridge-like features oriented in the normal direction to the substrate surface.

The effect of gelatin on the morphology of the zinc deposit was investigated by EBSD. As shown in Figure 4-10, the average grain size of feature (i) decreased from 5 μm to 3 μm as 2 mg/L gelatin was added. However, the large ridge-shaped features grew abnormally to an average size of 20 μm.

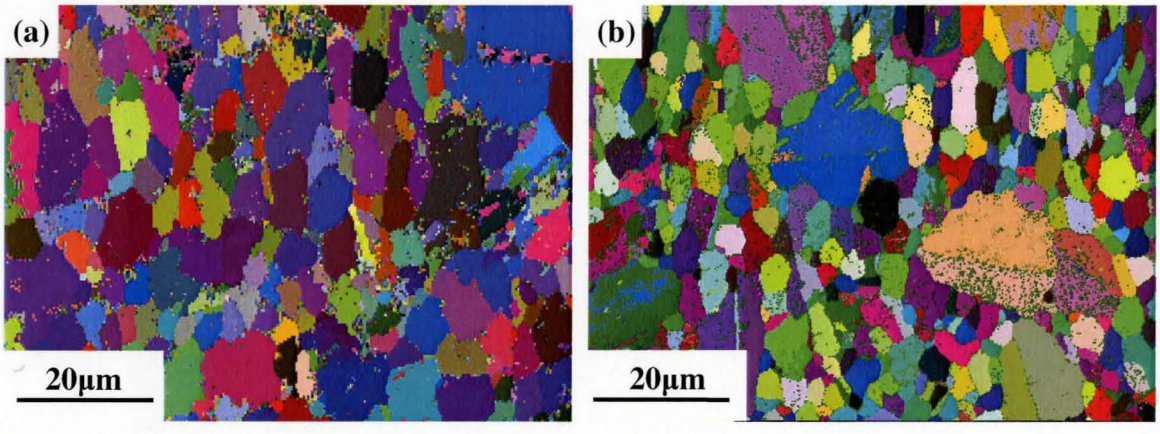

Figure 4-10: Effect of gelatin on the grain size of zinc coatings prepared using pH 3 electrolytes (a) no gelatin (b) 2 mg/L gelatin

4.2.2 Effect of Gelatin on the Preferred Orientation of Zinc Coatings

The effect of gelatin on the crystallographic texture of the zinc coatings was investigated by X-ray diffraction with a scanning rate of 1 °/min. The zinc coatings were prepared using electrolyte B with pH 3 at 20 mA/cm^2 for 20 mins. The concentration of gelatin was varied from 0 mg/L to 6 mg/L.

X-ray investigation shows that zinc deposits prepared using electrolytes containing no gelatin showed a predominant orientation of (0002) basal plane nearly parallel to the substrate surface and as the gelatin concentration increased to 6 mg/L, the zinc deposit was composed of a more randomly oriented crystallographic structure. To quantitatively describe the preferred orientation of the deposits, the extent of basal plane preferred orientation was evaluated by the ratio of relative intensity of the (0002) to $(10\bar{1}1)$ planes (R-ratio), as shown in Figure 4-11. It is seen that as the concentration of gelatin exceeded 4 mg/L, the value of the R ratio decreased from 128 to 1, which indicates a random crystallographic orientation for these deposits. It is also seen from Figure 4-11, that the deposits prepared using pH 3 electrolytes have stronger basal plane preferred orientation than those prepared using pH 5 electrolytes.

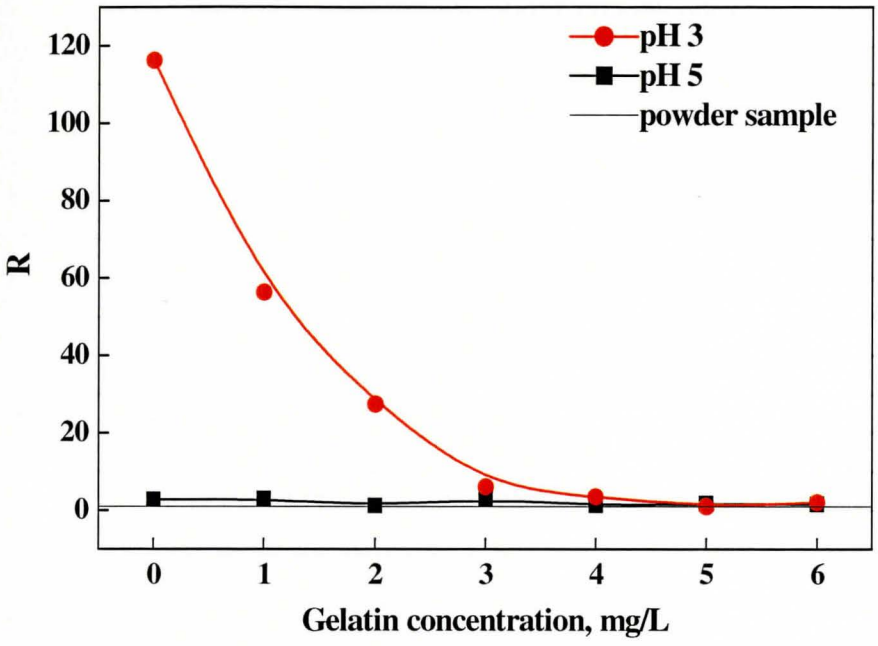

Figure 4-11: Ratio of the relative intensity of (0002) to $(10\bar{1}1)$ versus gelatin concentration in electrolytes

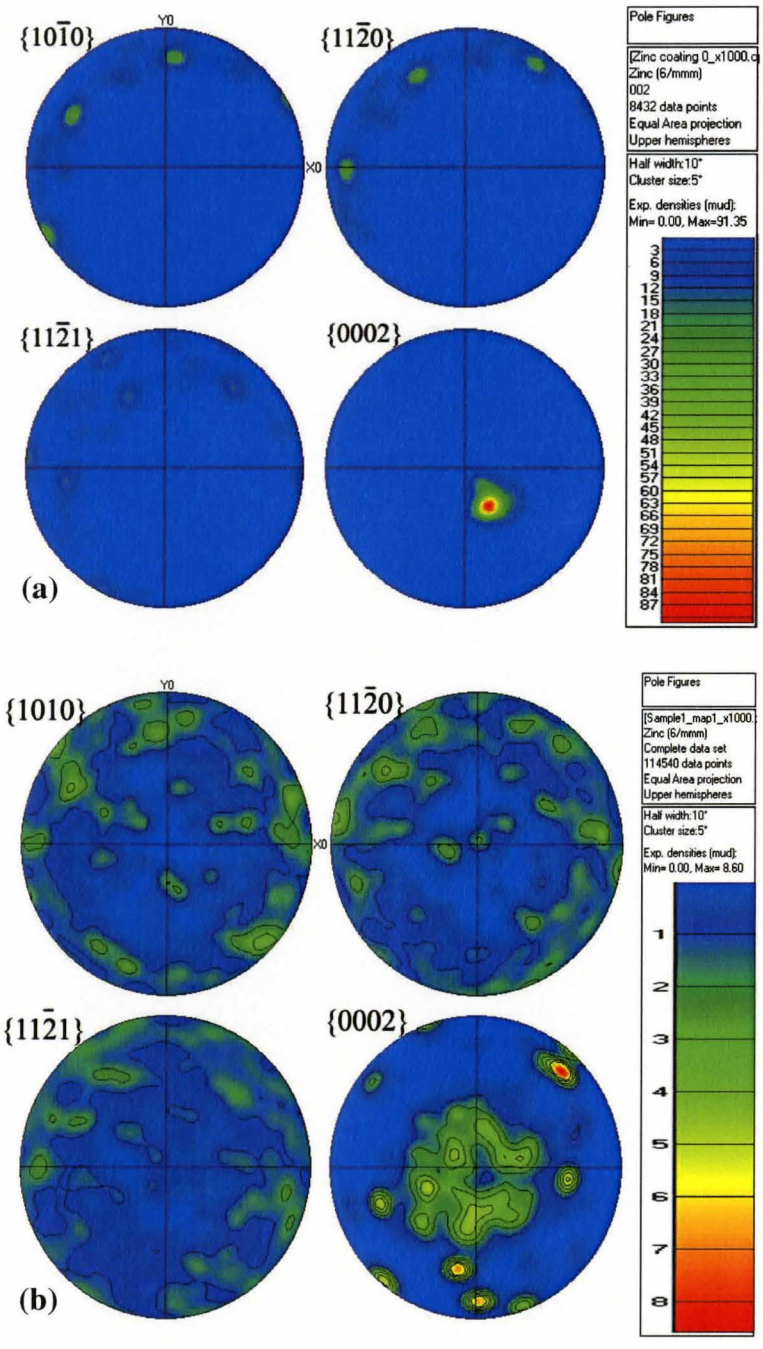

Figure 4-12: Pole figures of zinc coatings obtained from pH 3 electrolytes (a) no gelatin and (b) 2 mg/L gelatin

The crystallographic orientation of the zinc deposits was also examined by using EBSD. The pole figures in Figure 4-12 present different crystallographic orientations in samples from electrolytes containing no gelatin and 2 mg/L gelatin. In the sample without gelatin, basal plane exhibited high intensity and the pyramid faces had very weak intensity. Thus, the zinc deposit showed a basal plane preferred orientation; while for the sample with 2 mg/L gelatin, the intensity of basal plane reflections decreased and the diffraction of pyramid faces were enhanced. This result was consistent with those of X-ray diffraction.

4.2.3 Effect of Gelatin on the Microhardness of Zinc Coatings

The microhardness of zinc coatings prepared from electrolyte B with pH 3 was assessed as a function of gelatin concentration. The results are shown in Figure 4-13. The microhardness increased with gelatin concentration to 3 mg/L, becoming constant for higher gelatin concentrations.

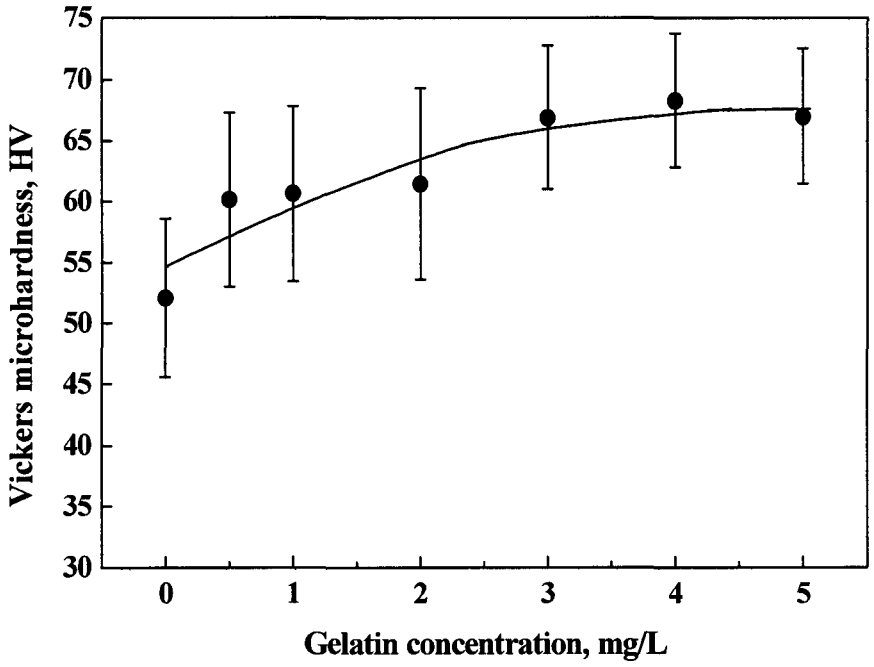

Figure 4-13: Microhardness versus concentration of gelatin for coatings deposited using pH 3 electrolytes

4.2.4 Effect of Gelatin on Potentiodynamic Polarization Behaviour of Zinc Coatings

The potentiodynamic polarization behaviour of zinc coatings made using electrolyte B with pH 3 was investigated. It was found, as shown in Figure 4-14, that there was no significant difference between the potentiodynamic polarization curves of zinc coatings made from electrolytes containing different concentrations of gelatin.

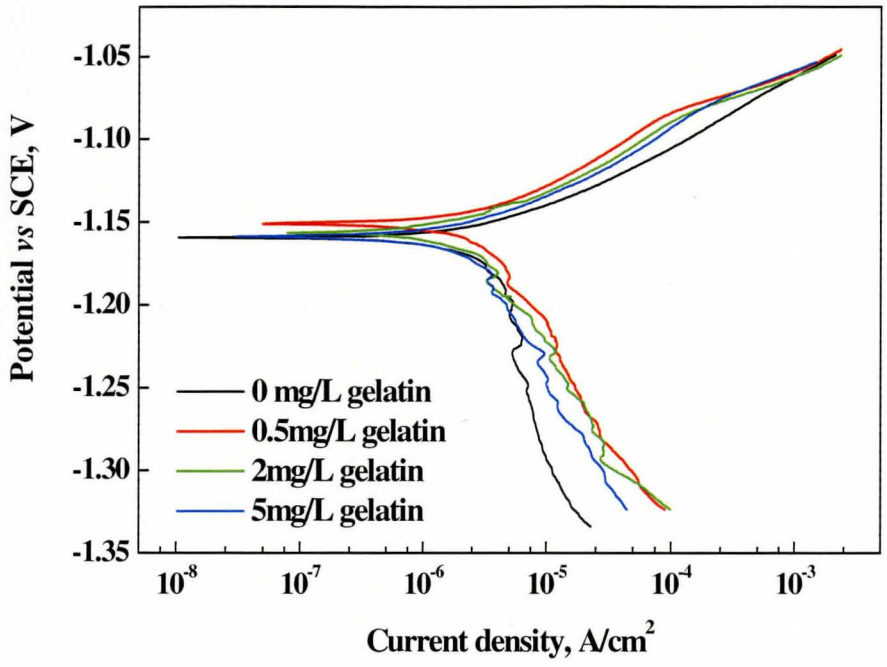

Figure 4-14: Tafel curves of zinc coatings as a function of gelatin concentration in pH 3 electrolytes

4.2.5 Investigation on the Functional Mechanism of Gelatin

To obtain a better understanding of the effects of gelatin on the zinc cathodic electrodeposition process, the cathode polarization behaviour of the substrate in deposition electrolytes was measured. The potential of substrate was measured versus gelatin concentrations in electrolyte B with pH 3. As shown in Figure 4-15, the cathode potential decreased with an increase in electrolyte gelatin concentration.

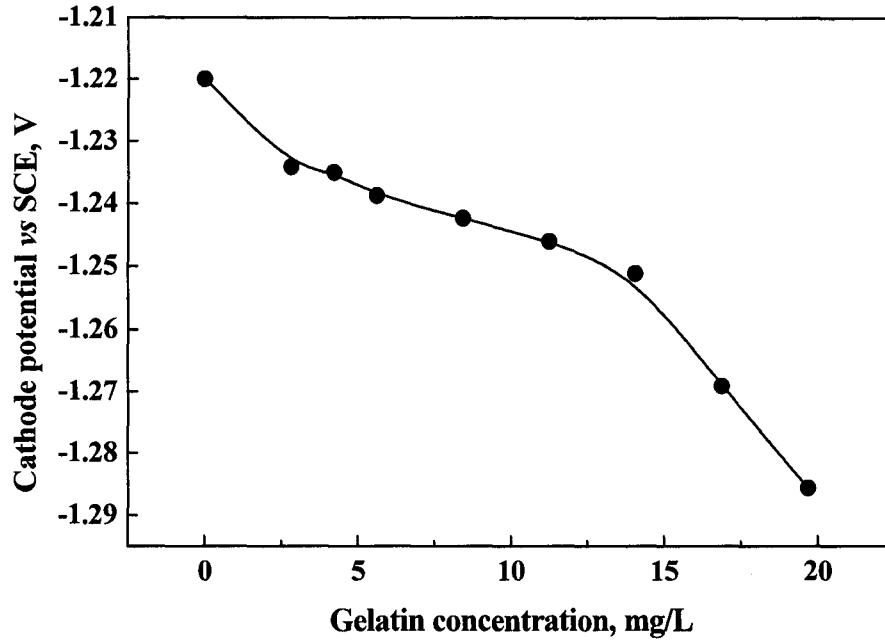

Figure 4-15: Cathode potential versus gelatin concentration

Figure 4-16 shows cathode polarization curves for the experimental stainless steel substrates in zinc sulphate solutions at pH 5, pH 3 and pH 3 containing 2 mg/L gelatin. The cathode polarization of stainless steel was carried out from the open circuit potential to -2.0V versus the SCE. According to the results, zinc reduction occurred at potentials below -1.1V versus the SCE. The variation in pH value of the electrolytes exhibited no significant influence in the cathode polarization behaviour for the stainless steel within the zinc reduction potential range, since curves (a) and (b) are insignificantly different. The addition of gelatin to the solution at pH 3 decreased the current density of cathode

polarization, which indicates that zinc reduction was inhibited and that zinc deposited at a lower rate.

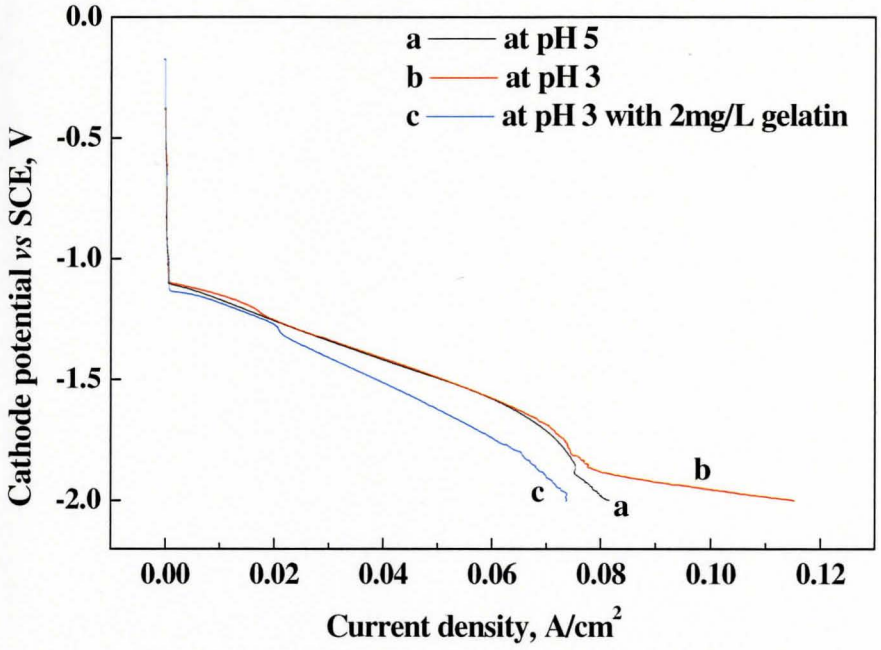

Figure 4-16: Cathode polarization curves for coated samples in zinc sulphate solutions with (a) pH 5, (b) pH 3 and (c) pH 3 containing 2 mg/L gelatin

4.3 Electrodeposition of Zinc and Yttria Stabilized Zirconia (YSZ) Particles

Although having superior self-sacrificial corrosion properties, pure zinc exhibits relatively low wear resistance, resulting in the formation of scratches and breaks within the coating. Consequently, the protective properties of the coatings are degraded as these

discontinuities increase in size. To improve the mechanical performance of the deposits, composite coatings of zinc and ceramic phases were developed. Yttria fully stabilized zirconia (YSZ) particles were added to the deposition electrolytes with no or 2mg/L gelatin, designated as electrolytes C and D, as shown in Table 3-1. The morphology of the composite coatings, the distribution of particles within the zinc matrix and the properties of the composite coatings were investigated and will be discussed in this section.

4.3.1 Morphology of Composite Coatings and Particle Distribution

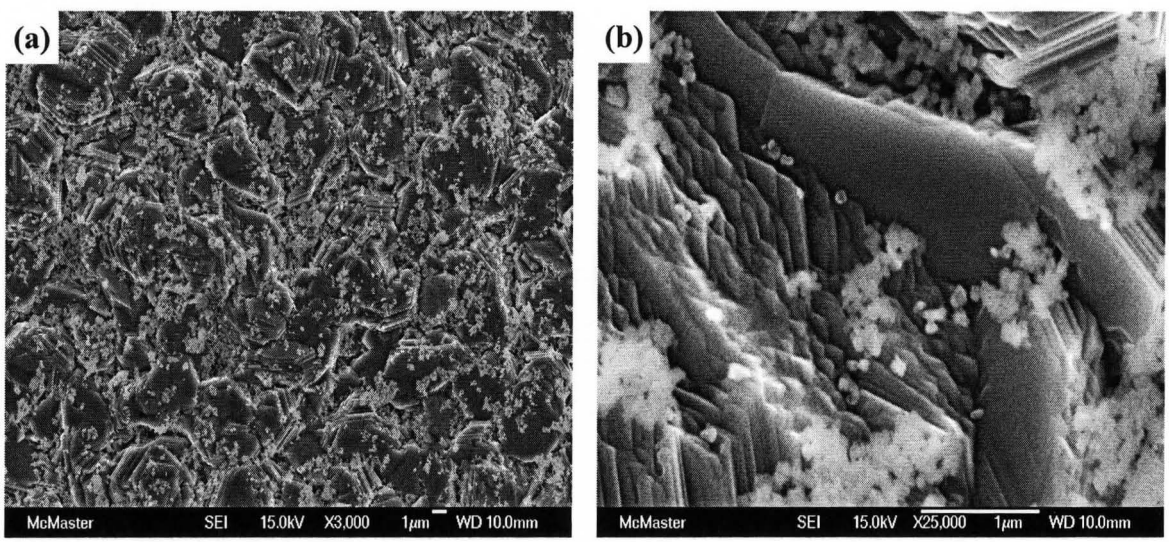

Figure 4-17: Morphology of composite coating prepared using pH 3 electrolyte containing 5 g/L YSZ particles: (a) low magnification (b) high magnification

Figure 4-17 shows the morphology of the composite coating and the distribution of YSZ particles in the zinc deposit. Most of the ceramic particles rest preferentially on the edges

and macrosteps of the growing zinc layers and a few ceramic particles were randomly deposited on the surface of the zinc layer.

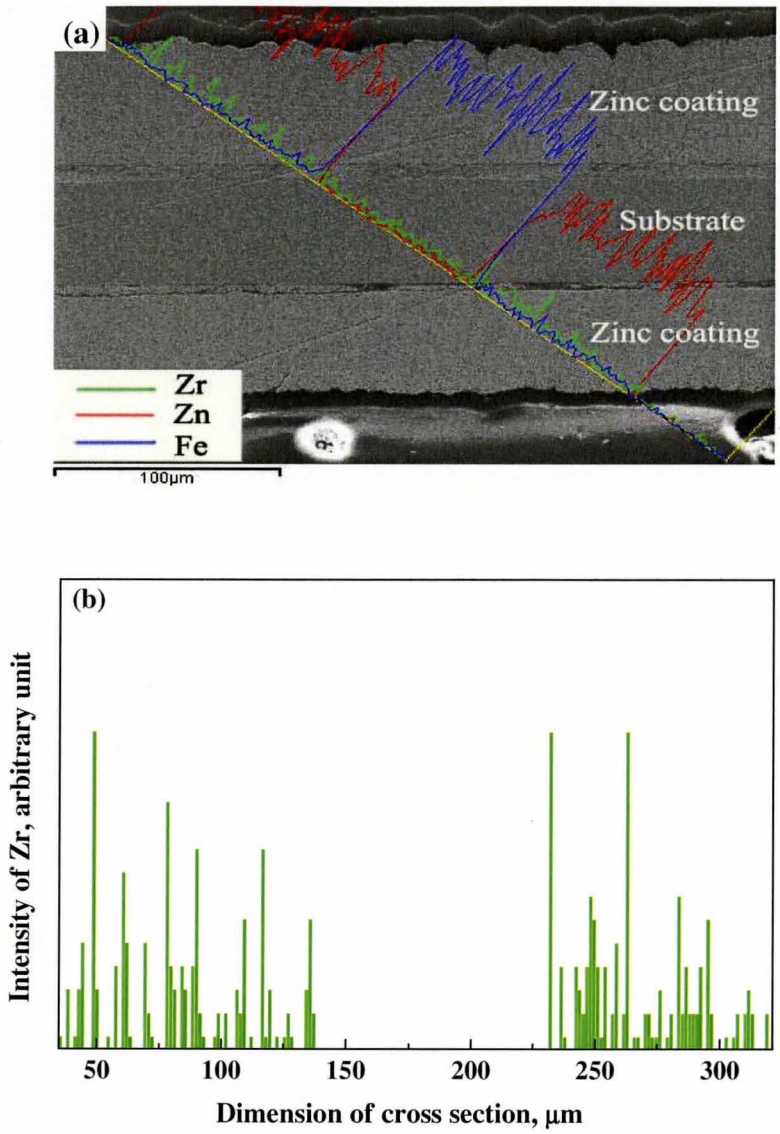

Figure 4-18: Elemental line scanning spectrum in the cross section of a coated sample. The coating was deposited using pH 3 electrolyte containing 15g/L YSZ particles.

The distribution of YSZ particles in the zinc matrix along the direction perpendicular to the substrate surface was investigated using an EDS elemental linear scan, as shown in Figure 4-18. A discontinuous but un-preferential signal for zirconium was detected along the scanning direction. There was no significant variation in the relative intensity of the zirconium signal from different depths of the matrix which indicates that the ceramic particles were distributed randomly through the coating in the perpendicular direction of the substrate surface.

Investigation on the fracture cross section also showed a random distribution of YSZ particles in the zinc matrix, as shown in Figure 4-19.

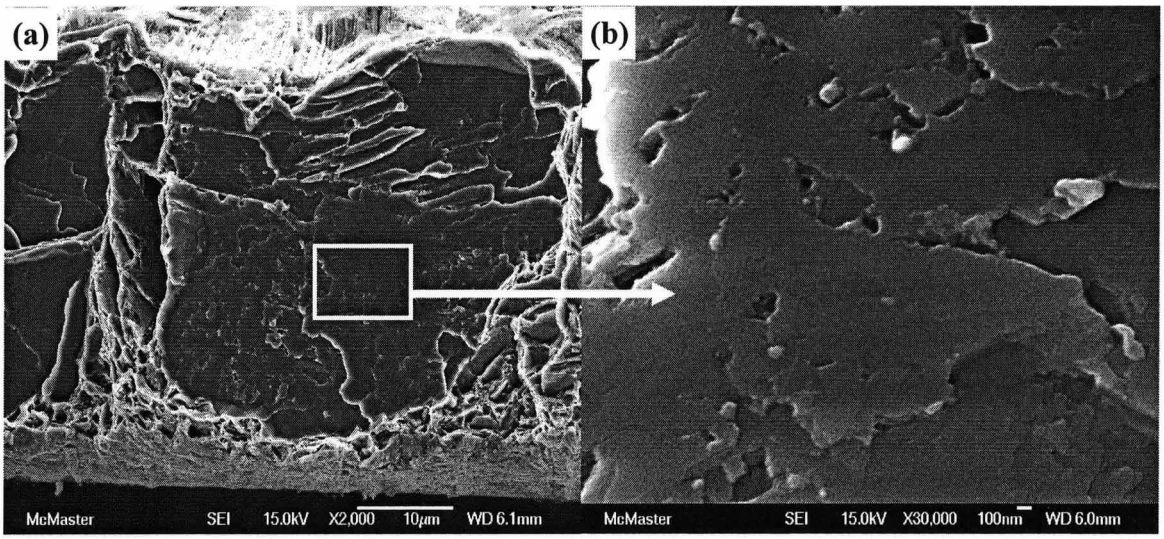

Figure 4-19: Fracture cross section of composite coating prepared using pH 3 electrolyte containing 15g/L YSZ particles: (a) low magnification and (b) high magnification

The incorporation of YSZ ceramic particles into the zinc matrix from coatings fabricated using electrolytes C and D was examined using SEM. The results are shown in Figure 4-20, Figure 4-21, and Figure 4-22, indicating that the incorporation of ceramic particles into the composite coatings was strongly influenced by the composition of the electrolyte.

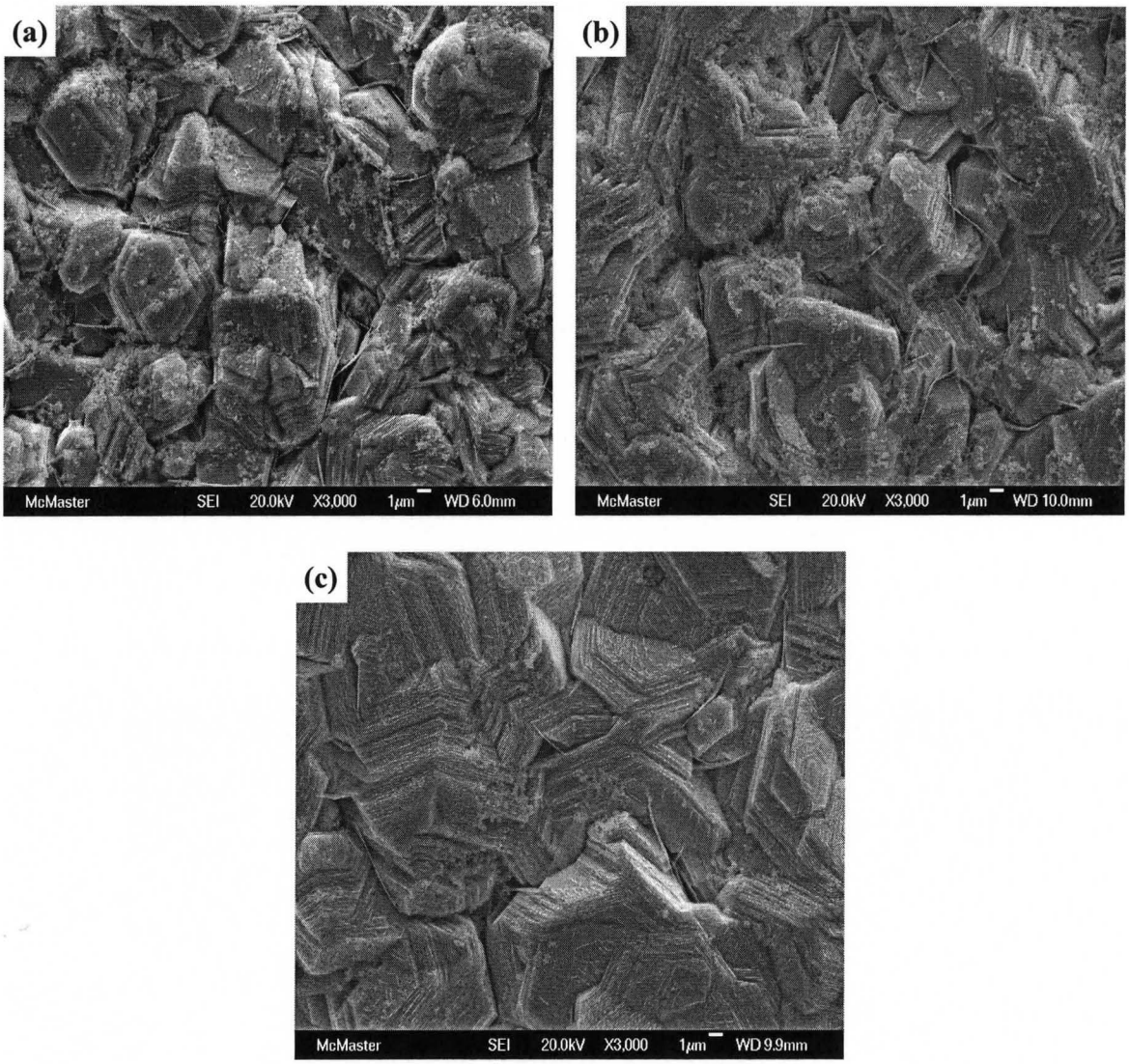

Figure 4-20: Morphology of composite coatings prepared using pH 5 electrolytes with various concentrations of YSZ particles (a) 2 g/L, (b) 5 g/L, (c) 10 g/L

Figure 4-20 shows the morphology of composite coatings prepared from electrolyte C with pH 5. Very few YSZ particles were incorporated into the zinc matrix prepared using the pH 5 electrolyte.

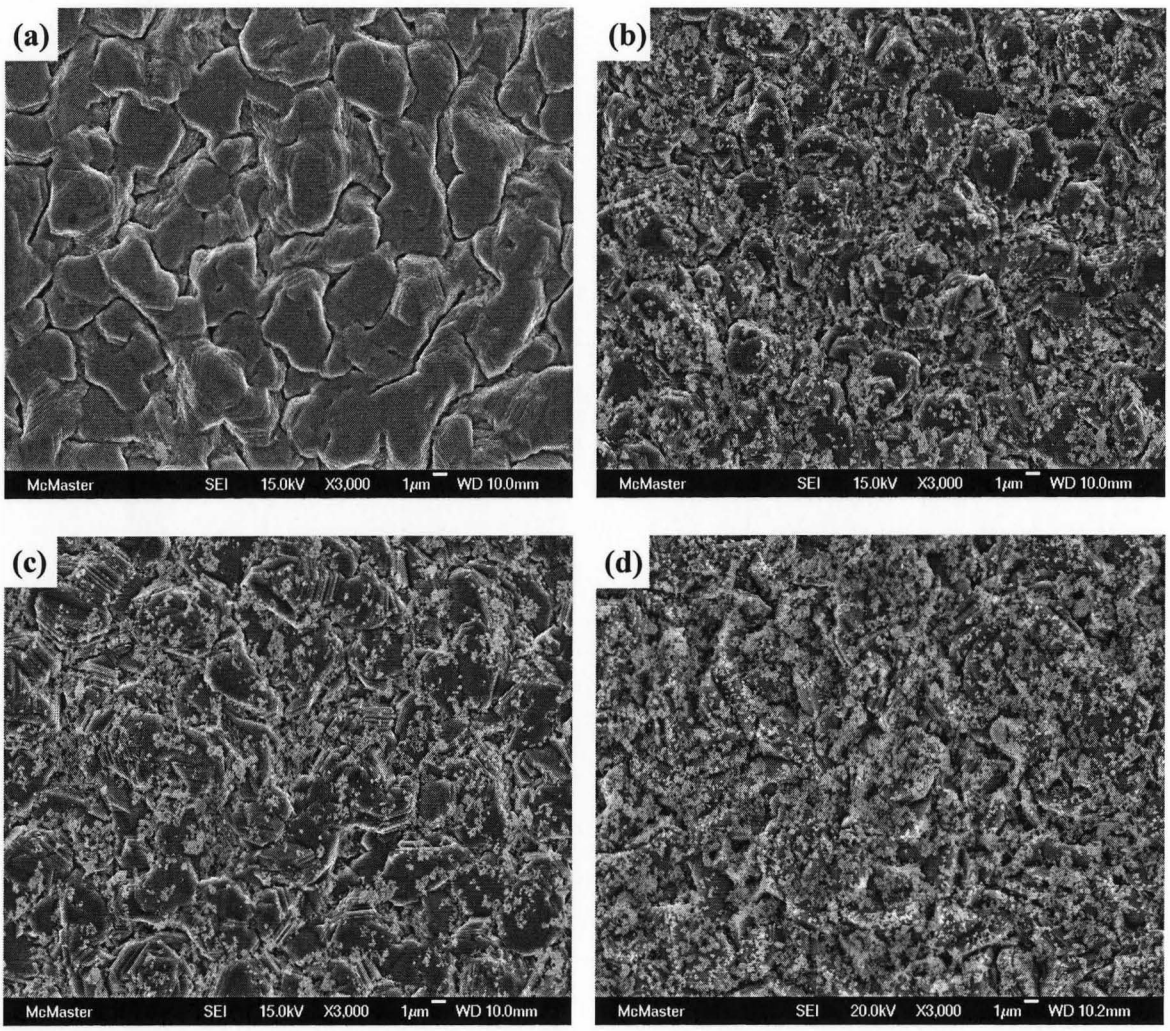

Figure 4-21: Morphology of composite coatings prepared using pH 3 electrolytes with various concentrations of YSZ particles (a) 2 g/L, (b) 5 g/L, (c) 10 g/L, (d) 15 g/L

For the composite coatings produced from electrolyte C with pH 3, particle concentrations in the deposit increased with increasing particle concentration in the electrolyte with or without the addition of gelatin, as shown in Figure 4-21 and Figure 4-22. However, it was seen from the SEM images that with the increase in particle concentration in the electrolytes, the particles appeared to agglomerate.

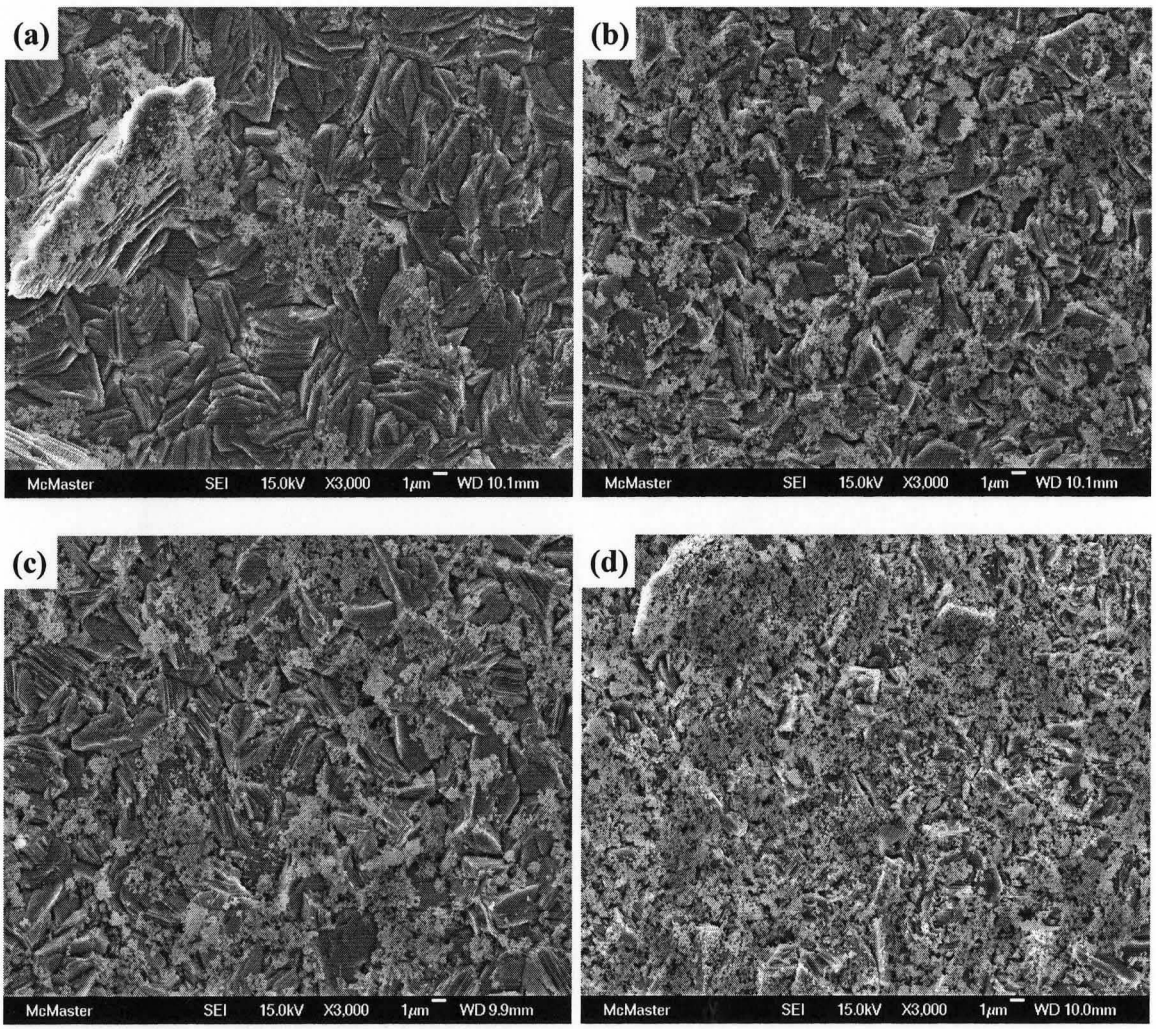

Figure 4-22: Morphology of composite coatings prepared from electrolyte D with various concentrations of YSZ particles (a) 2 g/L, (b) 5 g/L, (c) 10 g/L, (d) 15 g/L

The volume fraction of YSZ particles in composite coatings obtained from electrolytes C and D were estimated using EDS mapping. The incorporation of ceramic particles in the zinc deposits was characterized as a function of the particle concentration in the electrolyte. The results are plotted in Figure 4-23. As indicated in this figure, with the same particle concentration in the electrolyte, more YSZ particles were deposited from pH 3 electrolytes and suspensions containing gelatin. The enhancement in co-deposition of ceramic particles from these two suspensions was attributed to the higher mobility of the ceramic particles.

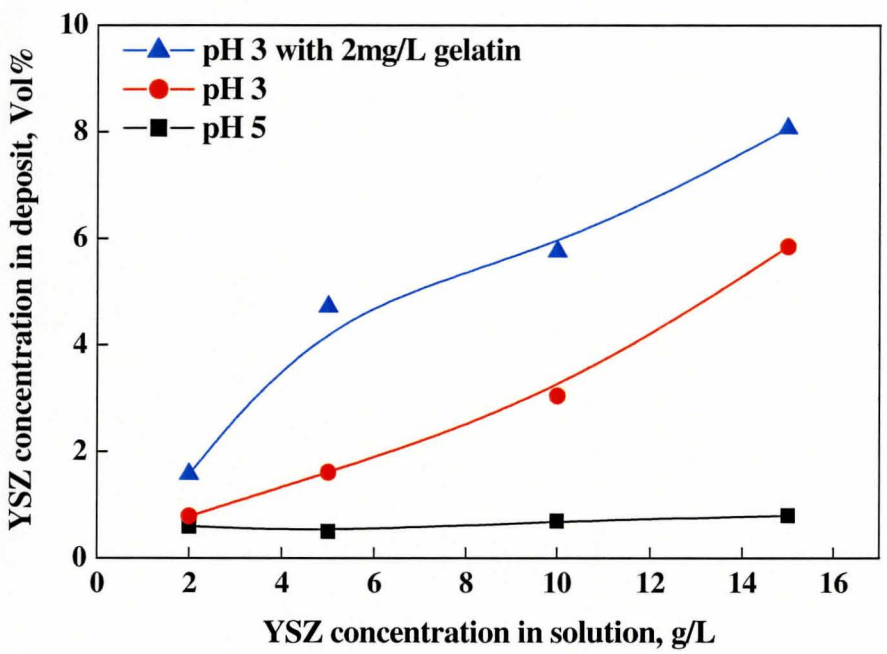

Figure 4-23: Volume fraction of YSZ particles in the zinc deposit versus YSZ concentration in the solution

4.3.2 Properties of Composite Coatings

The incorporation of ceramic particles in the zinc matrix was aimed at improving the mechanical properties of the zinc coatings. Materials with higher hardness normally exhibit higher anti-wear performance, therefore, the Vickers microhardness of the composite coatings without gelatin and with 2 mg/L gelatin were assessed as a function of the concentration of YSZ particles in the electrolyte. The average values of 20 measurements on each sample are plotted in Figure 4-24. The results show that the microhardness of the composite coatings increased with the incorporation of YSZ particles into the zinc deposit when the particle concentration was less than 5 g/L and became constant above this value. With the same particle concentrations in the suspension, the composite coatings prepared from electrolytes containing gelatin exhibited higher microhardness values than those from electrolytes with no gelatin.

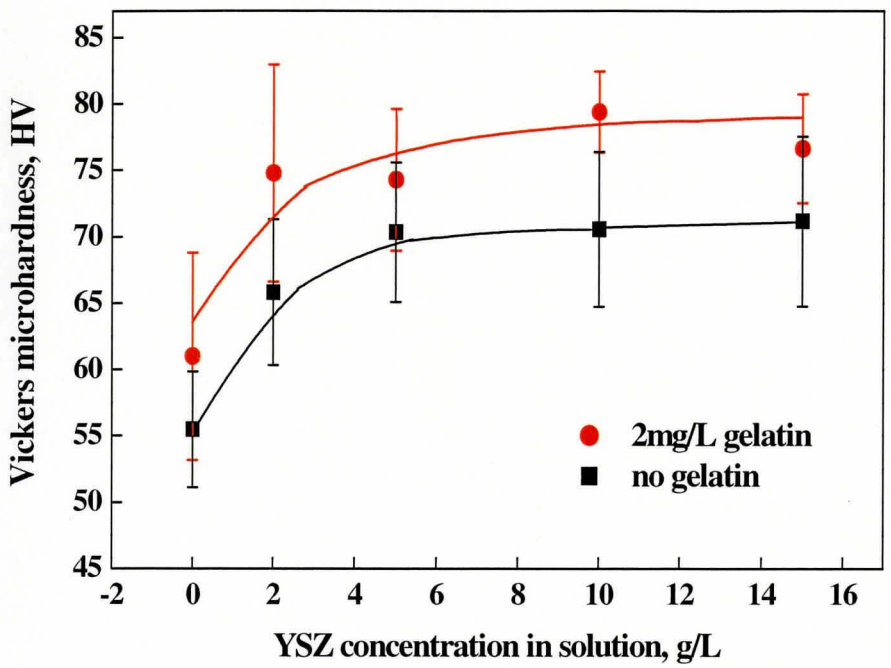

Figure 4-24: Vickers microhardness of the composite coatings

The anti-corrosion characteristics of composite coatings prepared from electrolytes containing 2 mg/L gelatin and various concentrations of YSZ particles were evaluated by potentiodynamic polarization tests. The measurements were performed in the potential range of ±250 mV from the open circuit potential vs. the SCE at a scan rate of 1 mV/s. As shown in Figure 4-25, the addition of inert ceramic particles moved the potentiodynamic polarization curves in the noble direction, i.e. the corrosion potential changed positively from -1.16 V in curve (a) to -1.11 V in curve (c) versus the SCE.

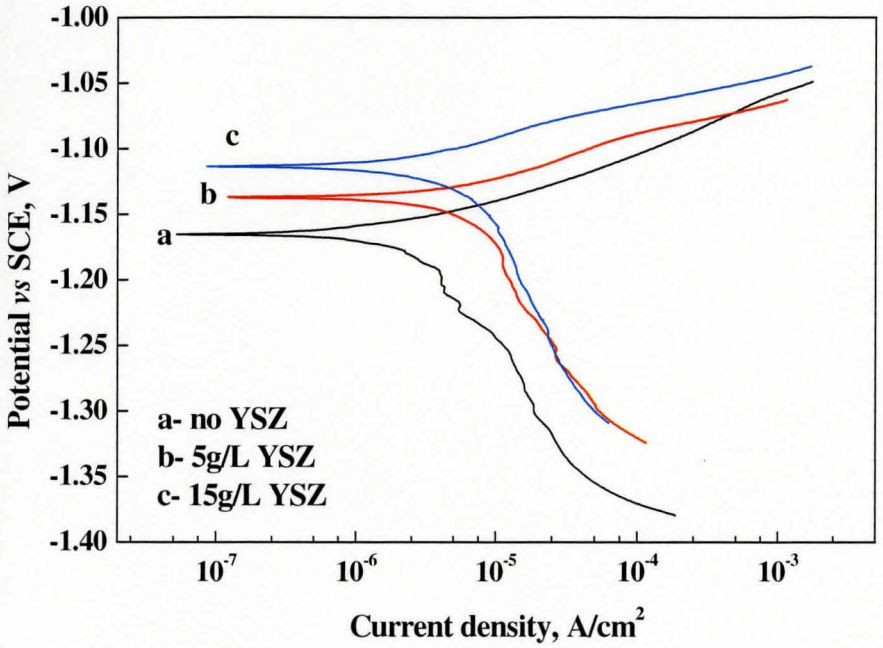

Figure 4-25: Potentiodynamic polarization curves of composite coatings

4.3.3 Investigation of Co-deposition Mechanism

The cathode polarization of stainless steel substrates was also carried out in electrolytes containing 5 g/L YSZ particles at pH 5 and pH 3 and for an electrolyte containing 5 g/L YSZ particles with 2 mg/L gelatin at pH 3. The stainless steel foils were polarized from their open circuit potential to -2.0V versus the SCE. As the voltage scanned negatively, the response current was recorded and is shown in Figure 4-26. At a given cathode potential, the current density for zinc reduction decreased with decreasing pH of the electrolytes (curve (b) versus curve (a)) and slightly decreased with the addition of gelatin to the electrolyte (curve (c) versus curve (b)).

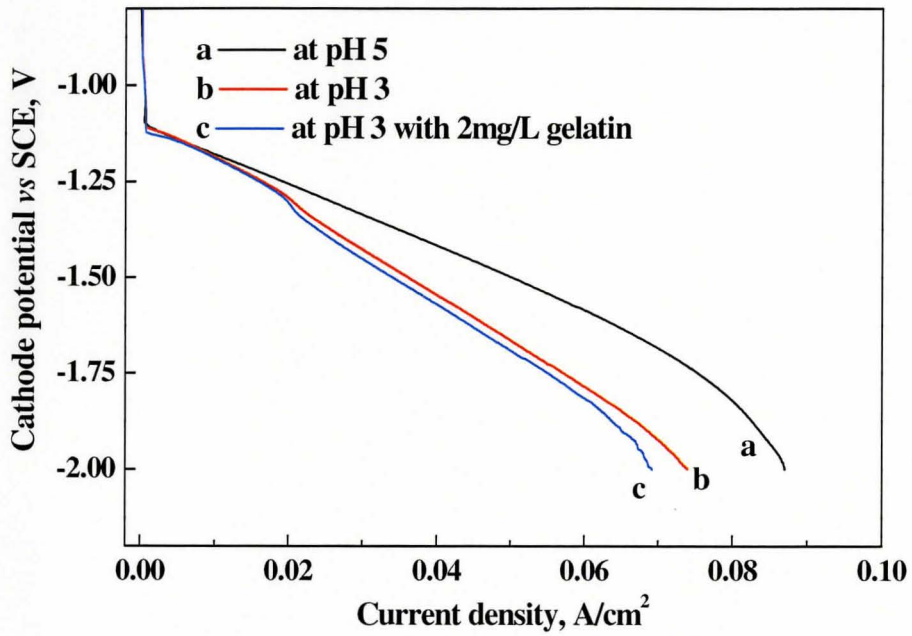

Figure 4-26: Cathode polarization curves from electrolytes containing 5 g/L YSZ particles at (a) pH 5, (b) pH 3 and (c) pH 3 containing 2 mg/L gelatin

5 DISCUSSION

5.1 Effects of Operating Parameters on the Electrodeposition of Zinc

5.1.1 Current Density

To obtain high quality coatings, the deposition time and current density were varied as outlined in Table 3-2. Figure 4-1 indicated that the deposit weight was linearly related to the deposition time, and for a given deposition time, increased with current density.

It is clear from the result that the electrodeposition behaviour of zinc follows Faraday's law, which can be expressed as:

$$w = MIt / nF \tag{5-1}$$

Where, w is the weight gain at the electrode surface per unit area (g/cm^2), M is the molar mass of the deposited metal, I is the current density, t is the deposition time, n is the number of electrons transferred for metal reduction and F is the Faraday constant. Here, for the electrodeposition of certain metal, i.e. with a given M and n, the deposition rate is directly related to the current density. With constant current density, the deposit grows linearly with time. In the electrodeposition process with acidic electrolytes, due to the hydrogen evolution, the current efficiency would be less than 100%. Thus, the real deposit weight would be proportional to the value calculated from the Faraday's law.

5.1.2 Deposition Time

As shown in Figure 4-2 and Figure 4-3, the zinc grain size increased with deposition time. The image of the coating cross-section, as shown in Figure 4-3 (d), exhibited a columnar microstructure composed of uniform fine grains next to the substrate surface and coarse columnar grains at a further distance from the substrate. The development of such a microstructure can be interpreted by growth competition between adjacent grains[19]. It is suggested that different crystal faces grow at different rates. The faces with lower surface energy grew faster than ones with higher surface energy and the faster growing faces would expand laterally and cover the slower growing faces adjacent to them, forming coarse columnar grains i.e. the lower surface energy faces grew at the expense of the higher surface energy faces. A schematic image describing the development of this columnar structure is shown in Figure 5-1[19].

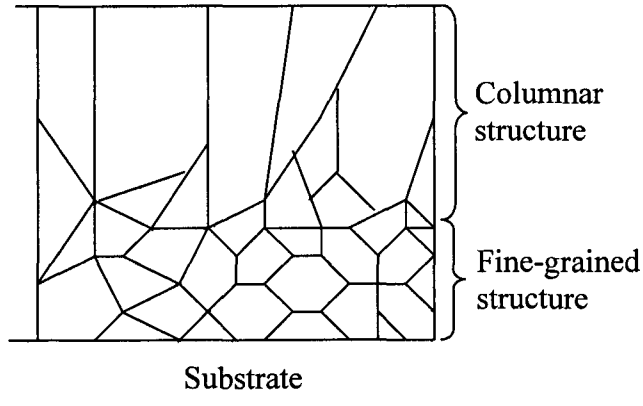

Figure 5-1: Schematic cross section of a columnar deposit[19]

The competitive growth of crystal planes is also suggested to cause the texture development in the electrodeposited coatings to form a microstructure with the observed preferred orientation of crystal faces having lower surface energy[19]. In our case, the growth of basal plane (0002) was enhanced by the deposition process i. e. the R ratio increased with deposition time and current density, as shown in Figure 4-4.

The formation of basal plane preferred orientation may be generated from preferred nucleation at the beginning of the deposition process or growth process during subsequent deposition. For the former case, the texture of the substrate is supposed to have an affect on the nucleation process, which needs further investigation. However, in this study, it is reasonable to assume that samples in Figure 4-4 have the same condition for nucleation, since they were prepared in the same deposition system and on the same kind of substrates. Thus, the enhancement of basal plane preferred orientation in the subsequent deposition process could be attributed to the preferential growth of the close-packed basal plane (0002) which has lower surface energy in the hexagonal zinc crystal.

5.1.3 Electrolyte pH

The electrolyte pH exerted a pronounced influence on the morphology and crystallographic orientation of the zinc deposit. As Figure 4-5 and Figure 4-6 showed, zinc deposits prepared from electrolytes with pH 3 had a homogeneous appearance. The microstructure consisted of finer, compact zinc hexagonal layers with a basal plane preferred orientation.

In cathode electrodeposition from acidic electrolytes, the prime side reaction is hydrogen reduction on the cathode surface. Hydrogen evolution is completed through the following two stages involving an intermediate state of discharged hydrogen atoms adsorbed on the metal surface[67]:

$$H^+ + e = H_{ads} \tag{5-2}$$

$$2H_{ads} = H_2 \quad \text{or} \quad H^+ + H_{ads} + e = H_2 \tag{5-3}$$

Hydrogen ions have been suggested to preferentially adsorb on activated sites related to zinc nucleation and incorporation into the lattice, and inhibit the deposition and growth of zinc[21]. Thus hydrogen evolution can cause a significant change in the crystallization and growth of a zinc deposit. Furthermore, if hydrogen ions were preferentially reduced on the top of protrusion sites of the deposit with higher electric field intensity, they could retard the deposition of zinc on these sites and promote the formation of a smoother coating surface.

On the other hand, the adsorption of hydrogen ions on the cathode surface would lead to an increase in cathode overpotential. In the Helmholtz double layer model, the potential distribution in the vicinity of the cathode surface can be described using the model shown in Figure 5-2[16].

For cathodic zinc deposition, the electrode potential has to be more negative than the potential in the equilibrium state i.e. having a higher overpotential. The activation overpotential of the cathode can be described by the equation:

$$\eta = -\frac{RT}{(1-\beta)zF}\ln\left(\frac{i_c}{i_0^o}\right) - \left(\frac{\beta}{1-\beta}\right)\psi_1 \tag{5-4}$$

where the η is the activation overpotential, the i_c is the net cathodic deposition current, i_0 is the equilibrium exchange current density across the double layer, z is the number of valence electrons and β is the symmetry factor of the activation polarization energy hump.

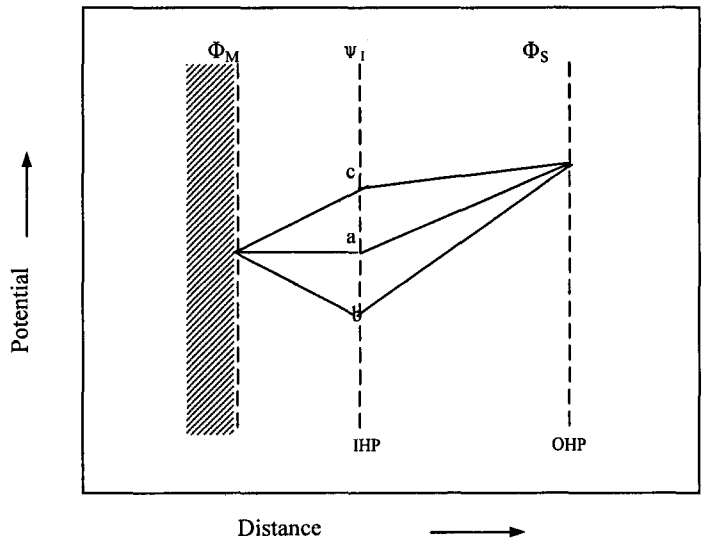

Figure 5-2: Simplified model of the potential distribution in the Helmholtz double layer (a) with no specific adsorption, (b) with cations specifically adsorbed in the inner Helmholtz plane, (c) with anions specifically adsorbed in the inner Helmholtz plane [16], here IHP is the inner Helmholtz plane, OHP is the outer Helmholtz plane and ψ_1 is the potential at the inner Helmholtz plane.

In the case of cationic adsorption, the potential at the inner Helmhotlz plane ψ_1 is positive and the overpotential has a more negative value, i.e. the cathode overpotential increases. The nucleation rate increases with the cathode overpotential, resulting in grain refinement of zinc deposits prepared from solutions with lower pH, as shown in Figure 4-5.

The increase in overpotential could also result from the adsorption of hydrogen gas bubbles on the cathode surface. The adsorbed hydrogen bubbles occupied a fraction of the surface area, diverting part of the electric current in this area to adjacent region and increasing the local current density. The redistribution of current density caused an increase in the activation overpotential in the vicinity of the gas bubbles and resulted in the refinement of grain size and alteration of the orientation of the crystallographic planes, as shown in Figure 4-5 and Figure 4-6.

5.2 Effects of the Gelatin on the Electrodeposition of Zinc

In acidic solutions, zinc deposition is completed by the reduction of zinc ions via the two-stage reaction in equation 2-1. The high exchange current in the zinc discharge reaction and simultaneous hydrogen evolution often results in the formation of incoherent deposits with gas pits. Thus, organic additives are normally employed to alter the hydrogen reduction rate and improve the deposit quality. In our case, gelatin was added to the zinc sulphate solution in order to reduce hydrogen gas evolution.

5.2.1 Functional Mechanism of Gelatin

It was shown that small amounts of gelatin additives change the structural characteristics of the deposit in Figure 4-8 and Figure 4-9. The pronounced effects of gelatin on cathodic zinc deposit is related to its molecular structure[17]. As a high protein polymer, gelatin is a heterogeneous mixture of amino acids (glycine, proline or hydroxyproline and serine) linked by peptide chains $-CO-NH-$. The structural unit of gelatin is shown in Figure 5-3. In electrolytes, gelatin is hydrolyzed and takes on a positive or negative charge depending on the acidity of the solution[23]. In acidic media, the positive charge of the gelatin molecule is primarily related to the amino groups on the side chains (the circled part in Figure 5-3), which preferentially adsorb on the cathode surface via the amino end groups[25].

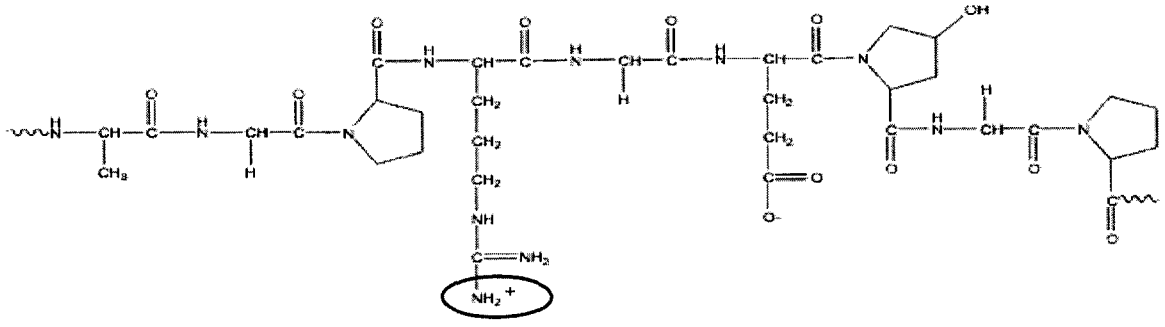

Figure 5-3: Structural unit of gelatin[23]

The adsorption of positively charged gelatin macromolecules on the cathode surface, similar to the effect of cationic adsorption, moved the cathode potential negatively and increased the cathode overpotential. Cathode potential was measured as a function of

gelatin concentration in the zinc sulphate solution with pH 3 as shown in Figure 4-15. The cathode potential moved in the negative direction with an increase in gelatin concentration due to the adsorption of gelatin molecules on the cathode surface. According to the literature[23], gelatin is a zwitterionic polymer and its isoionic point is pH 7.0 to 9.0 depending on the configuration of the gelatin molecule. In solutions with pH lower than the isoionic point, a greater positive charge and higher mobility of gelatin molecules with a reduction in solution pH would be expected[23]. Thus, under the same electric field strength, more gelatin molecules were adsorbed on the cathode surface in the pH 3 solution versus the pH 5 solution.

The interaction between gelatin molecules and the cathode surface was investigated through the cathode polarization behaviour of the stainless steel substrates in solutions without and with 2 mg/L gelatin. The results were shown in Figure 4-16. As the cathode potential scanned in the negative direction, zinc reduction started at the potential of -1.1 V versus the SCE, resulting in the observed abrupt increase in current density. It is seen that, at a given cathode potential, the polarization curve measured for the solution containing 2 mg/L gelatin with pH 3 (curve c) had the lowest current density, indicating that zinc discharge was inhibited by the adsorbed gelatin layer. This phenomenon is consistent with the results in Figure 4-15. The adsorbed gelatin molecules covered the cathode surface and the growing surface of the deposited zinc, competed for activated sites with the arriving zinc ions and prevented zinc ion reduction.

In acidic media, gelatin inhibited hydrogen gas evolution during the electrodeposition process. Hydrogen evolution was accomplished through two stages as shown in reactions 5-2 and 5-3. The competition for activated sites was not only between gelatin molecules and zinc ions but also between gelatin and hydrogen ions. The adsorbed gelatin molecules occupied activated sites for the reduction of hydrogen ions and decreased the reaction rate for reaction 5-2. Moreover, the adsorbed gelatin molecules constrained the diffusion of hydrogen atoms to the cathode or the deposit and retarded the completion of reaction 5-3.

5.2.2 Modification of Coating Microstructure

In the deposits prepared from pH 5 electrolytes, the less effective adsorption of gelatin on the cathode surface lead to the formation of an inferior deposit consisting of large hexagonal zinc platelets, as shown in Figure 4-8.

The interaction between gelatin macromolecules and cathode surface in pH 3 electrolytes significantly changed the microstructure of the zinc deposit. As Figure 4-9 showed, dense zinc deposits with small grains were prepared from pH 3 electrolytes containing gelatin. The structure of the zinc deposit changed from large hexagonal basally oriented platelets to small ridge-shaped flakes as the gelatin concentration increased from 0.5 mg/L (Figure 4-9(a)) to 6 mg/L (Figure 4-9(d)). As seen in these figures, the zinc grains tended to present a bimodal distribution: fine grains with an average grain size of 3 μm and coarse

ridge-shaped structures with an average size of 20 μm in the longitudinal axis. Each coarse ridge-shaped structure was composed of zinc layers growing with the basal plane normal to the substrate. The number of the ridge-shaped structures increased with the gelatin concentration. It is suggested that the formation of these coarse structure was due to the local adsorption of gelatin molecules.

The development of this microstructure can be explained by the out growth mode of zinc deposition[27] and is shown schematically in Figure 5-4. It is known that as soon as a current was applied, the electric field would cause the redistribution of zinc ions in the area close to the cathode surface. The consumed zinc ions were replaced by ones from the bulk solution through migration in the solution and diffusion across the double layer of the cathode surface. If the rate of refreshment of zinc ions was lower than the consumption, the concentration of zinc ions would drop at the electrode and form an ion deficient area in the vicinity of the cathode. The resultant increase in cathode overpotential would expand the ion deficient area. Consequently, the growing tips of the deposit could meet with higher zinc ion concentration than the lateral surface could, and then they would grow at a higher rate in the normal direction to the substrate surface. In the present study, the adsorption of gelatin on the cathode surface increased the cathode overpotential, hindering the diffusion of zinc ions to the cathode surface, promoting the deposition of zinc in the out growth mode as illustrated in Figure 5-4, resulting in the formation of the ridge-shaped microstructure. SEM images of the zinc deposit in Figure 4-2 (b) are also included in Figure 5-4 for comparison.

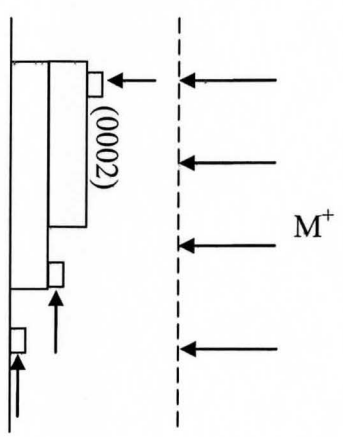

Low overpotential

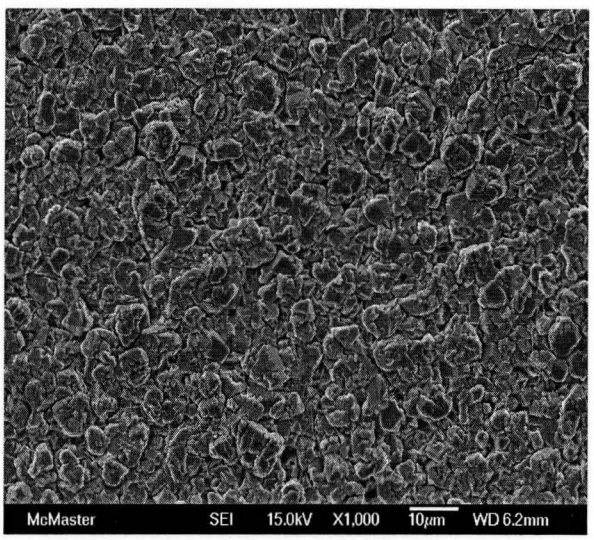

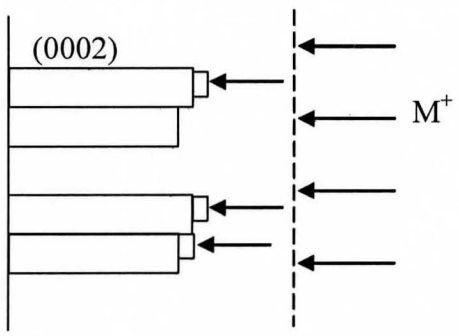

High overpotential

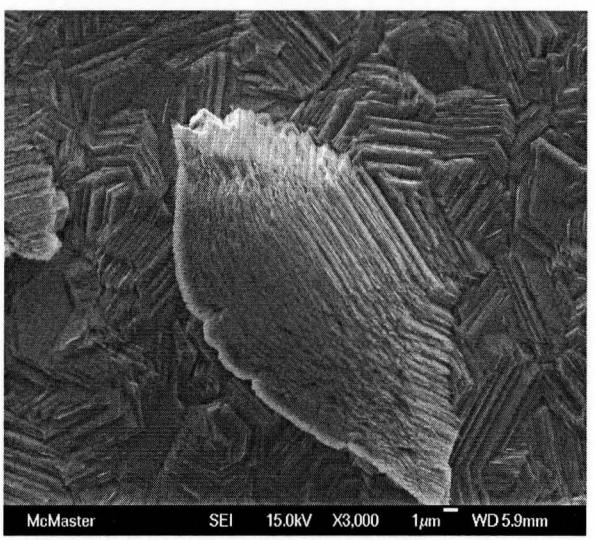

Figure 5-4: Growth modes of zinc deposit under various cathode overpotentials[27]

The out growth mode would be responsible for the observed modification in the crystallographic texture of the deposit as well. The growth of the zinc deposit in the vertical direction caused a decrease in the fraction of the basal plane oriented nearly parallel to the substrate surface, as shown in Figure 4-11 and Figure 4-12. In Figure 4-11

the ratio of the basal plane (0002) to the pyramid face $(10\bar{1}1)$ X-ray peak was equal to 1 when the gelatin concentration exceeded 4 mg/L, which means the preferred orientation of the basal plane completely disappeared. In Figure 4-12, the angle between the basal plane and the substrate surface, measured using the Wulff net, was 25° for the deposit with no gelatin, and 75° for that prepared using the electrolyte containing 2 mg/L gelatin. The variation of the angle means that as the gelatin concentration increased, the basal plane rotated from the direction nearly parallel to the substrate surface to the one almost perpendicular to the substrate surface.

5.2.3 Effects of Gelatin on the Mechanical and Electrochemical Properties of the Deposit

The addition of gelatin also had influence in the mechanical and electrochemical properties of the zinc deposit. As shown in Figure 4-13, coating microhardness increased with gelatin concentration in the electrolyte. This result is related to the crystallographic orientation of the zinc deposit.

It is well known that zinc exhibits anisotropic mechanical properties due to its hexagonal crystal structure i.e. the crystallographic orientation has considerable influence in the mechanical properties. In hexagonal zinc crystal, deformation is accomplished via slip on the $\{0001\}$ basal planes along the $\langle 11\bar{2}0 \rangle$ directions. It was reported by Mei et al[I 68] that slip on the basal plane became difficult when the deformation axis was parallel or normal

to the basal plane. Thus, zinc deposits having orientations other than normal to the basal plane exhibited higher resistance to deformation due to the limitations of basal slip. For the deposits prepared with gelatin, the increase in microhardness was a result of the decrease of basal plane orientation parallel to the substrate surface. Gelatin itself has also been suggested to be responsible for increasing the microhardenss of the deposit[69]. In the process of deposition, the gelatin adsorbed on the cathode surface may be incorporated into the zinc deposit depending on the relative rates of zinc deposition and gelatin desorption. If the zinc deposited more rapidly than gelatin desorbed, the gelatin would be incorporated into the zinc deposit. It has been observed that amino compounds can increase the hardness of electrodeposited coatings[69]. Sekar and Jayakrishnam[12] also reported that the addition of gelatin had a hardening effect on zinc coatings produced using acetate acid electrolytes.

The addition of gelatin caused no appreciable changes in the electrochemical properties of the zinc deposit as assessed by the potentiodynamic polarization tests in Figure 4-14. From the literature[70], zinc coatings' electrochemical properties are closely related to their crystallographic orientation. The corrosion rate of different crystallographic planes was considered to increase in the sequence of $(0001) < (11\bar{2}0) < (10\bar{1}0)$. The higher corrosion resistance observed was due to the higher bonding energy of the atoms in the close-packed plane. In our case, the more noble corrosion potential was also observed for deposits which had a strong basal-plane preferred orientation, as shown in Figure 4-7. However, the addition of gelatin inhibited the growth of the basal plane and affected the

potentiodynamic polarization behaviour negatively. On the other hand, inhibition of hydrogen evolution by gelatin promoted the formation of a uniform, non-porous zinc deposit and effectively increased the coating's corrosion resistance. Therefore, in summary, the addition of gelatin affected the electrochemical properties of the zinc deposit in two contrary ways, resulting in the observed unappreciable change in the potentiodynamic polarization curves.

5.3 Co-deposition of Composite Coatings of Zinc and YSZ Particles

Our results showed that the addition of gelatin brought very limited improvement in coating properties. With the objective of improving the mechanical and electrochemical properties of electrodeposited Zn-based coatings, YSZ particles were added to the deposition electrolytes and Zinc/YSZ composite coatings were prepared using the electrodeposition technique.

YSZ is an advanced ceramic material and has been extensively studied in this decade[62, 71]. It has a unique combination of mechanical and electrochemical properties including excellent thermal stability, high fracture toughness and superior corrosion resistance. In particular, the thermal expansion coefficient of YSZ is close to that of steel, which makes YSZ an excellent candidate for the strengthening phase in metal-based composite materials.

5.3.1 Distribution of YSZ Particles and the Co-deposition Mechanism

Figure 4-17, Figure 4-18 and Figure 4-19 show the morphology of the composite coatings and the distribution of YSZ particles on the coating surface and through the cross-section of the deposit. Figure 4-17(b) shows that in the surface parallel to the substrate, the YSZ particles distributed in two ways: some ceramic particles were randomly deposited on the surface of the zinc layers, and most particles rested preferentially on the edges and macrosteps of the growing zinc layer. As seen in the images of the cross section, Figure 4-18 and Figure 4-19, the YSZ particles were incorporated randomly throughout the cross section of the deposit.

This distribution was due to the lower bonding energy needed for the ceramic particles to incorporate into the zinc deposits on the macrosteps and sidewalls of the zinc layer than on the flat surface. The edges and steps were also activated sites for incorporation of zinc atoms into the lattice. Thus, the co-deposition process was a competition between the placement of zinc and ceramic particles for the activated sites.

According to Guglieimi's mechanism[63] for the co-deposition of metal and ceramic particles, the ceramic particles were first loosely adsorbed on the growing zinc surfaces. Through charge transfer with the electrode, the adsorbed particles were then chemically bonded to the local site. As the arriving zinc ions were continuously reduced, the ceramic particles were pushed to boundary areas by the incorporation of deposited zinc ions into

the lattice. When two zinc crystals intersected, the ceramic particles were entirely trapped in the zinc deposit.

For particles incorporated into the bulk of the zinc deposit, the MTM model[64] can offer a better explanation. YSZ particles have been observed to be positively charged in aqueous solutions and the point of zero charge is pH 6[71]. The particles are positively charged at pH less than 6. In the present study, the solution pH was 3. Thus, when a particle was dispersed in an electrolyte, a cloud of positively charged ions formed around it. Some zinc ions were also included in the ionic cloud. Once the particle with its surrounded ions arrived at the cathode, the zinc ions were reduced and incorporated into the deposit. When a certain number of the zinc ions were reduced, the ceramic particle was captured.

5.3.2 Incorporation of Ceramic Particles into the Zinc Deposit

A prerequisite for the co-deposition of metals and ceramic particles is the formation of stable suspension of ceramic particles[40, 41, 45]. The factors affecting the stability of a suspension were discussed in Chapter 2. In our case, incorporation of YSZ particles was investigated in three electrolytes: zinc sulphate solutions containing 2-15 g/L YSZ particles with pH 5, the same suspension but with pH 3 and the pH 3 electrolyte containing 2 mg/L gelatin.

As shown in Figure 4-23, the incorporation of YSZ particles was more efficient in the pH 3 and gelatin containing electrolytes. This result suggested that hydrogen ions and gelatin

molecules increased the mobility of the YSZ particles and promoted the formation of a stable suspension. Electrophoretic deposition[32] requires the development of the appropriate surface charge on the ceramic particles. The common representation of particle surface charge is the zeta potential, which determines the mobility of ceramic particles. In another words, a higher zeta potential is desired for successful deposition of ceramic particles. As mentioned in last section, in aqueous solutions, the zeta potential of YSZ versus pH was measured by Moreno et al.[71], in which the point of zero charge (PZC) for YSZ was determined to be approximately pH 6. As the pH values in the present investigation were lower than 6, the zeta potential is supposed to be positive, as shown in Figure 2-5. Thus, in acidic solutions, a positive charge was developed on the ceramic particle surfaces by the adsorption of hydrogen ions, increasing the mobility of the YSZ particles and their deposition rate. However, yttria dissolves in strong acid solutions, so the pH of the deposition solutions had to be controlled in a moderate range.

The addition of gelatin to the electrolytes was also found to promote the co-deposition of ceramic particles. This might be due to the electrosteric stabilization of ceramic particle suspensions by gelatin adsorption. Generally, it is difficult to stabilize particles in solutions of metal salts due to their high ionic strength, which reduces the thickness of the double layer of the ceramic particles[32, 33]. As gelatin was added, it was protonated and positively charged in the acidic environment[46]. The protonated gelatin macromolecules adsorbed on the ceramic particle surfaces, promoting electrosteric stabilization of the ceramic particles, which is less sensitive to high ionic strength. At the same time, the

adsorbed layer of gelatin molecules positively charged the ceramic particles, promoting their movement to the cathode under the force of the electric field.

The effects of pH and gelatin on the co-deposition of YSZ particles were studied via the cathode polarization method, and the results are shown in Figure 4-26. As indicated by the results, at a given cathode potential, the current density for zinc reduction decreased with decreasing electrolyte pH (curve b versus curve a) and slightly decreased with the addition of gelatin to the solution (curve c versus curve b). The inhibition of zinc deposition in the latter two cases (b and c) was the result of competition between zinc ions and YSZ particles for activated deposition sites at the cathode, i.e. the deposited YSZ particles blocked the incoming zinc ions and prevented them from reducing at the cathode, resulting in the observed decrease in zinc reduction current. However, since there was no direct observation of the adsorption of gelatin, the mechanism of interaction between the YSZ particles and gelatin molecules is not thoroughly understood, and further investigation is required.

5.3.3 Mechanical and Electrochemical Properties of Zinc/YSZ Composite Coatings

The Vickers microhardness of the composite coatings deposited from pH 3 electrolytes without gelatin and with 2 mg/L gelatin was assessed as a function of the concentration of YSZ particles in the electrolyte. The results were shown in Figure 4-24. The increase

in hardness of the coatings was attributed to the dispersion strengthening effect of the ceramic particles in the zinc matrix. The constant microhardness as the particle concentrations exceeded 5 g/L is suggested to be caused by the agglomeration of ceramic particles in the deposit. Although these agglomerated particles were deposited on the cathode under the force of the applied electric field and agitation, they lost their dispersion hardening effect due to the large size of the agglomerates.

With the same particle concentration in the suspension, the higher microhardness of the composite coatings prepared from electrolytes containing gelatin was attributed to the effect of gelatin on the incorporation of YSZ particles into the zinc matrix as discussed above and the alteration of the texture of the zinc matrix.

The corrosion characteristics of composite coatings with various concentrations of YSZ particles were evaluated by potentiodynamic polarization of the composite coatings in a sodium chloride solution. The improvement in corrosion resistance of the composite coatings, as shown in Figure 4-25, arose from two effects of the ceramic particles: as inert and insulating materials, the YSZ particles protect the underlying zinc matrix against corrosion attack, essentially forming a localized barrier film. The corrosion current decreased with increasing concentration of YSZ particles in the deposit due to the larger areas covered by the particles. On the other hand, according to the research of Satoshi[72], the incorporated ceramic particles could also support corrosion products and slow down subsequent corrosion rate of the metal, also by a local barrier mechanism.

6 CONCLUSIONS AND RECOMMENDATIONS

6.1 Conclusions

In summary, the above study consisted of three parts:

1. Electrodeposition of pure zinc coatings using zinc sulphate electrolytes. In this part, the effects of processing variables, such as the current density, deposition time and pH on the quality of the zinc deposit were studied.
2. Electrodeposition of zinc coatings using zinc sulphate solution with the addition of gelatin. The effects of gelatin on the microstructure, crystallographic orientation and mechanical and electrochemical properties of the zinc deposit were investigated as a function of gelatin concentration in the electrolytes.
3. Co-deposition of zinc and YSZ ceramic particles. The mechanisms of co-deposition of zinc and ceramic particles were studied. Incorporation of ceramic particles in the zinc matrix and the properties of the composite coatings were also determined as a function of the particle concentration in the suspensions. In this part, the effects of pH and gelatin on the incorporation of ceramic particles were discussed.

Based on the results and discussion, the following conclusion can be drawn:

In the gelatin free electrolytes:

1. Operating parameters had significant effects on the electrodeposition process and the quality of the deposit. The deposition rate was controlled by the current density and the deposition rate increased with current density. As the deposition time increased,

the microstructure changed from uniform fine grains adjacent to substrate to coarse, columnar grains.

2. The decrease in solution pH effectively refined the grain size of the zinc deposit, promoting the basal plane preferred orientation and resulted in the improvement of the corrosion potential.

In electrolytes containing gelatin:

3. Gelatin profoundly affected the electrodeposition of zinc via adsorption of the gelatin molecules on the growing zinc deposit surface, effectively inhibiting hydrogen evolution.
4. The presence of gelatin considerably altered the morphology of the deposit in the pH 3 electrolyte and resulted in the formation of a microstructure with a bimodal grain size. The adsorption of gelatin promoted the out growth mode and resulted in the formation of a ridge-shaped microstructure.
5. As the gelatin concentration increased, the preferred orientation of basal plane was inhibited, increasing the microhardness of the zinc deposit.
6. The addition of gelatin into the deposition electrolytes showed no significant effect on the potentiodynamic polarization behaviour of the zinc deposits.

In the co-deposition of zinc and YSZ composite coatings:

7. Composite coatings of zinc and YSZ particles were prepared directly from zinc sulphate electrolytes containing dispersed YSZ particles.

8. The YSZ particles were preferentially distributed on the growing edges and macrosteps of the zinc deposit. The YSZ particles competed with zinc ions for activated deposition sites.
9. The co-deposition of YSZ particles was significantly enhanced by the reduction in pH and the addition of gelatin to the electrolyte.
10. The microhardness and anti-corrosion properties of conventional zinc coatings were improved by the addition of YSZ particles.

6.2 Recommendations for Further Work

1. Further investigate the functional mechanism of the gelatin using electrochemical methods such as cyclic voltammetry.
2. Measure the zeta potential of YSZ particles in solutions with different pH and containing gelatin to further study the stabilization mechanism of the ceramic particles.
3. Study the impedance of the pure zinc and zinc/YSZ composite coatings to investigate the corrosion properties of these coatings.
4. Measure the wear resistance of zinc/YSZ composite coatings.

REFERENCES

1: Xiaoge Gregory Zhang. *Corrosion and Electrochemistry of Zinc.* Plenum, New York. (1996) : 7.

2: Mordechay Schlesinger and Milan Paunovic. *Modern Electroplating,* fourth edition, John Wiley & Sons, Inc., Pennington, New Jersey. (2000): 424.

3: T. G. Sitnikova and A. S. Sitnikov. "The Effect of Organic Additives on the Kinetics of Zinc Electroplating". Protection of Metals, Vol. 41, No. 6, (2005): 607-609.

4: C. A. Loto, I. Olefjord and H. Mattsson. "Surface Effects of Organic Additives on the Electrodeposition of Zinc on Mild Steel in Acid-Chloride Solution". Corrosion Prevention & Control, No. 8, (1992): 82-88.

5: T. C. Franklin. "Some Mechanisms of Action of Additives in Electrodeposition Process". Surface and Coatings Technology, No. 30, (1987): 415-428.

6: L. Oniciu and L. Muresan. "Some Fundamental Aspects of Leveling and Brightening in Metal Electrodeposition". Journal of Applied Electrochemistry, No. 21, (1991): 565-574.

7: D. Aslanidis, J. Fransaer and J. P. Celis. "The Electrolytic Codeposition of Silica and Titania Modified Silica with Zinc". Journal of the Electrochemical Society, Vol. 144, No. 7, (1997): 2352-2357.

8: V. John. "The Production of the Zinc-Silica Dispersion Coatings". The Use and Manufacture of Zinc and Zinc Alloy Coated Sheet Steel Products into the 21st Century (GALVATECH'95). The Iron and Steel Society (1995): 249-262.

9: A. Gomes, M. I. da Silva Pereira and M. H. Mendonca. "Zn-TiO_2 Composite Films Prepared by Pulsed Electrodeposition". Journal of Solid State Electrochemistry, No. 9, (2005): 190-196.

10: V. A. Paramonov and V. V. Levenkov. "Production of Antomobile Sheet with Coatings". Metallurgist, Vol. 48, No. 9-10, (2004): 473-477.

11: C. Kerr, D. Barker and F. Walsh. "Electrolytic Deposition (Electroplating) of Metals". Trans IMF, Vol. 80, No. 2, (2002): 67-72.

12: R. Sekar and Sobha Jayakrishnan. "Charateristics of Zinc Electrodeposits from Acetate Solution". Journal of Applied Electrochemistry, No. 36 (2006): 591-597.

13: Ernest W. Horvick. "Zinc in the World of Electroplating". Plating & Surface Finishing, No. 6, (2006): 42-48.

14: Kh. M. S. Youssef, C. C. Koch and P. S. Fedkin. "Influence of Additives and Pulse Electrodeposition Parameters on Production of Nanocrystalline Zinc from Zinc Chloride Electrolytes". Journal of the Electrochemical Society, Vol. 151, No. 2, (2004): 103-111.

15: Milan Paunovic and Mordechay Schlesinger. *Fundamentals of Electrochemical Deposition.* A Wiley-Interscience Publication, New York (1998): 109.

16: J. M. West. *Electrodeposition and Corrosion Process*. Van Nostrand Reinhold Company, London (1970): 33.

17: T. Ohgai, H. Fukushima, N. Baba, and T. Akiyama. "Effect of Polymer Additives on Zinc Electrowinning". Proceedings of the TMS Fall Extraction and Processing Conference, Pittsburgh, PA, USA, Lead-Zinc 2000: 855-963.

18: N. D. Nikolic, G. Novakovic, Z. Rakocevic, D. R. Durovic and K. I. Popov. "Comparative Reflection and Structural Analyses of Copper and Zinc Coatings Electrodeposited from Acid Sulfate Solution with and without Additives". Surface and Coatings Technology, No.298, (2002): 188-194.

19: M. Paunovic and M. Schlesinger. *Fundamentals of Electrochemical Deposition.* A Wiley-Interscience Publication, New York (1998): 123.

20: C. A. Loto and I. Olefjord. "Influence of Organic Additives on the Surface Characteristics of Zinc Electrodeposition on Mild Steel in Acid-Chloride Solution: pH, Bath-composition and Time-variation Effects". Corrosion Prevention &Control, No.12, (1992): 142-149.

21: Ki-Deok Song, Kwang-Bun Kim, Seong-Ho Han and Hongkee Lee. "Effect of Additives on Hydrogen Evolution and Adsorption during Zn Electrodeposition Investigated by EQCM". Electrochemical and Solid Letters, Vol. 7, No. 2, (2004): 20-24.

22: Fabio Galvani and Ivani A. Carlos. "The Effect of the Additive Glycerol on Zinc Electrodeposition on Steel". Metal Finishing, No.2, (1997): 70-72.

23: https://www.norlandprod.com/fishgel/hipure.html (2007-6-2)

24 : A. E. Saba and A. E. Elsherief. "Continuous Electrowinning of Zinc". Hydrometallurgy, No.54, (2000): 91-106.

25 : S. E. Afifi, A. R. Ebaid, M. M. Hegazy and A. K. Barakat. "The Effect of Additives on Zinc Deposit from Zinc Sulfate Solution". JOM, No.1, (1992): 32-34.

26: A. M. Alfantazi and D. B. Dreisinger. "The Role of Zinc and Sulfuric Acid Concentrations on Zinc Electrowinning from Industrial Sulfate Based Electrolyte". Journal of Applied Electrochemistry, No.31, (2001): 641-646.

27: Y. B. Yim, W. S. Hwang and S. K. Hwang. "Crystallographic Texture and Microstructure of Electrogalvanized Layer in Acid Sulfate Solution". Journal of Electrochemical Society, Vol. 142, No.8, (1995): 2604-2611.

28: J. H. Lindsay, R. F. Paluch, H. D. Nine, V. R. Miller and T. J.O'Keefe. "Interaction between Electrogalvanized Zinc Deposit Structure and the Forming Properties of Sheet Steel". Plating and Surface Finishing, Vol. 76, No. 3, (1989): 62-69.

29: Kazuo Kondo, Tomoya Murakami, Frank Cerwinski and Kunio Shinohare. "AFM Study on Morpholgy Evolution of Zinc Electrodeposits". ISIJ International Vol. 37, No. 2, (1997): 140-145.

30: H. Park and J. A. Szpunar. "The Role of Texture and Morphology in Optimizing the Corrosion Resistance of Zinc-based Electrogalvanized Coatings". Corrosion Science, Vol. 40, No. 4-5, (1998): 525-545.

31: A. Conde, J. De Damborenea. A. Duran and M. Menning. "Protective Properties of a Sol-gel Coating on Zinc Coated Steel". Journal of Sol-Gel Science and Technology, No.37, (2006): 79-85.

32 : I. Zhitomirsky. "Cathodic Electrodeposition of Ceramic and Organoceramic Materials. Fundamental Aspects". Advances in Colloid and Interface Science, No.97, (2002): 279-317.

33: Omer O. Van der Biest and Luc J. Vandeperre. "Electrophoretic Deposition of Materials". Annual Review of Materials Science, Vol. 29, (1999): 327-352.

34: M. E. Labib and R. Williams. "Experimental Comparison Between the Aqueous pH Scale and the Electron Donicity Scale". Colloid and Polymer Science, No.264, (1986): 533-541.

35: W. M. Sigmund, N.S. Bell and L. Bergstroem. "Novel Powder-processing Methods for Advanced Ceramics". Journal of the American Ceramic Society, Vol. 83, No. 7, (2000): 1557-1574.

36: N. L. Weise. Editor. *SME Mineral processing handbook*, Vol. 1, New York: Society of Mining Engineers, (1985): 42.

37: P. M. Biesheuvel and H. Verweij. "Theory of Cast Formation in Electrophoretic Deposition". Journal of the American Ceramic Society, Vol. 82, No. 6, (1999): 1451-1455.

38: M. E. Labib and R. Williams. "Use of Zeta-Potential Measurements in Organic Solvents to Determine the Donor-Acceptor Properties of Solid Surfaces". Journal of Colloid and Interface Science, Vol. 97, No.2, (1984): 356-366.

39: G. Wang, P. Sarkar and P. S. Nicholson. "Influence of Acidity on the Electrostatic Stability of Alumina Suspensions in Ethanol". Journal of the American Ceramic Society, Vol.80, No.4, (1997): 965-972.

40: B. V. Derjaguin and L. D. Landau. "A Theory of the Stability of Strolngly Charged Lyophobic Sols and of the Adhesion of Strongly Charged Particles in the Solution of Electrolytes". Acta Physicochim URSS, (1941): 633.

41: E. J. W. Verwey and J. Overbeek. *Theory of the stability of lyophobic colloids.* Ameterdam, Elsevier, (1948): 60.

42: X. Chu and D. T. Wasan. "Attractive Interaction Between Similarly Charged Colloidal Particles". Journal of Colloid and Interface Science, Vol. 184, No.1, (1996): 268-278.

43: E. Dickinson, L. Eriksson. "Particle Flocculation by Adsorbing Polymers". Advances in Colloid and Interface Science, Vol. 34, No. 1, (1991): 1-29.

44 : Friedrich Harbach and Hans Nienburg. "Homogeneous Functional Ceramic Components through Electrophoretic Deposition from Stable Colloidal Suspensions-I. Basic Concepts and Application to Zirconia". Journal of European Ceramic Society, No.18, (1998): 675-683.

45: J. Ma, R. Zhang, C. H. Liang and L. Weng. "Colloidal Characterization and Electrophoretic Deposition of PZT". Materials Letters Vol. 57, (2003):4648-4654.

46: Laxmidhar Besra and Meilin Liu. "A Review on Fundamentals and Applications of Electrophoretic Deposition (EPD)". Process in Materials Science, No.52, (2007): 1-61.

47: J. Fransaer, J. P. Celis and J. R. Roos. "Analysis of the Electrolytic Codeposition of Non-Bronwnian Particles with Metals". Journal of the Electrochemical Society, Vol. 139, No. 2, (1992): 413-425.

48: X. Pang, I, Zhitomirsky and M. Niewczas. "Cathodic Electrolytic Deposition of Zirconia Films". Surface & Coatings Technology, No.195, (2005): 138-146.

49: M. Giersig and P. Mulvaney. "Preparation of Ordered Colloid Monolayers by Electrophoretic Deposition". Langmuir, Vol. 9, No. 12, (1993): 3408-3413.

50: Y. Z. Wan, Y. L. Wang, H. M. Tao, G. X. Cheng and X. H. Dong. "Preparation and Characterization of Different Particles-copper Electrocomposites". Journal of Materials Science Letters, Vol.17, No. 15, (1998): 1251-1253.

51: S. Put, J. Vleugels, G. Anne and O. Van Der Biest. "Functionally Graded Ceramic and Ceramic-metal Composites Shaped by Electrophoretic Deposition". Colloids and Surfaces A: Physicochemical and Engineering Aspects, Vol. 222, No.1-3, (2003): 223-232.

52: K. Sato and K. Suzuki. "Diamond Occlusion Plating". Metal Finishing, Vol. 82, No.12, (1984): 21-26.

53: N. K. Shrestha, D. B. Hamal and T. Saji. "Composite Plating of Ni-P-Al_2O_3 in Two Steps and Its Anti-wear Performance". Surface and Coatings Technology, No.183, (2004): 247-253.

54: A. Moller and H. Hahn. "Synthesis and Charaterization of Nanocrystalline Ni/ZrO_2 Composite Coatings". NanoStructured Materials, Vol. 12 (1999): 259-262.

55: J. R. Roos, J. P. Celis, J. Fransaer and C. Buelens. "The Development of Composite Plating for Advanced Materials". JOM, Vol. 42, No.11, (1990): 60-63.

56: T. J. Tuaweri and G. D. Wilcox. "Behaviour of Zn-SiO_2 Electrodeposition in the Presence of N, N-dimethyldodecylamine". Surface & Coatings Technology, No.200, (2006): 5921-5930.

57: Z. Abdel Hamid. "Thermodynamic Parameters of Electrodeposition of Zn-Co-TiO_2 Composite Coatings", Anti-Corrosion Methods and Materials, Vol. 48, No.4, (2001): 235-240.

58: D. Aslanidis, J. Fransaer and J. P. Celis. "The electrolytic Codeposition of Silica and Titania Modified Silica with Zinc". Journal of the Electrochemical Society, Vol. 144, No.7, (1997): 2352-2357.

59: S. Hashimoto and M. Abe. "The Chatacterization of Electrodeposited Zn-SiO_2 Composites Before and After Corrosion Test". Corrosion Science, Vol. 36, No.12, (1994): 2125-2137.

60: W. Wang, H. T. Guo, J. P. Gao, X. H. Dong and Q. X. Qin. "XPS, UPS and ESR studies on the interfacial interaction in Ni-ZrO_2 composite plating". Journal of Materials Science, No.35, (2000): 1495-1499.

61: H. G. Kruger, A. Knote, U. Schindler, H. Kern and A. R. Boccaccini. "Composite ceramic-metal coatings by means of combined electrophoretic deposition and galvanic methods". Journal of Materials Science, No.39, (2004): 839-844.

62: G. N. K. Ramesh Bapu and S. Jayakrishnman. "Oxidation characteristics of electrodeposited nickel-zirconia composites at high temperature". Materials Chemistry and Physics, No.96, (2006): 321-325.

63: N. Guglielmi. "Kinetics of the Deposition of Inert Particles from Electrolytic Baths". Journal of the Electrochemical Society, Vol. 119, No. 8, (1972): 1009-1012.

64: J. P. Celis, J .R. Roos and C. Buelens. "A Mathematical Model for the Electrolytic Co-deposition of Particles with a Metallic Matrix". Electrochemical Science and Technology, Vol. 134, No. 6, (1987): 1402-1407.

65: ASTM, E 112-96: Standard Test Methods for Determining Average Grain Size, Section 3. Vol. 1, (2006): 273-297.

66 : ASTM, E 92-82: Standard Test Methods for Vickers Hardness of Metallic Materials, Section 3. Vol. 3, (2007): 291-299.

67: J. O'M. Bockris and S. U. M. Khan, *Surface Electrochemistry*, Plenum Press, New York (1993): 833.

68: Z. Mei and J. W. Morries. "Cracking of Textured Zinc Coating During Forming Process". A. R. Marder (Ed.), The Physical Metallurgy of Zinc Coated Steel, TMS, Warrendale, PA, (1994): 11-20.

69 : L. Grincevichene. "Influence of Inorganic Ion Species on the Electrodeposition of Zinc from Weak Acid Zinc Electrolytes". Metal Finishing, Vol. 93, No. 7, (1995): 10-14.

70: Raichevski, G. and Vitkova, St. "Influence of Incorporated Iodide Ions on the Electrochemiccal and Corrosion Properties of Electrolytic Deposits of Cobalt". Protection of Metals, Vol. 9, No. 6, (1973): 611-615.

71: R. Moreno, J. Requena and J. S. Moya. "Slip Casting of Yttria-stabilized Tetragonal Zirconia Polycrystals". Journal of the American Ceramic Society, Vol. 71, No.12, (1988): 1036-1040.

72: S. Hashi moto and Masaki Abe. "Characterization of Electrodeposited Zn-SiO_2 Composites Before and After Corrosion Test". Corrosion Science, Vol. 36, No. 12, (1994): 2125-2137.